Supporting Information

Extendend Materials and Methods

Animals

A BAC clone, RP23-443K20, that contains the translational start site of the *Epb41l5* gene was obtained from BACPAC Resources (http://bacpac.chori.org/), and targeting and control vectors were constructed as described. Following primers were used: the 32 bp p1 (5'-CAGAAAGTCGACGCTAGATCCCCTCGCCTACC-3') and 23bp p2 (5'-GGTGTGGGGTCTGGGAATGAAGG-3') to amplify the 2.5kb 5' arm of the targeting vector, the 19bp p3 (5'-GGTCAAACAGCTCCTGTCC-3') and 36bp p4 (5'-GACTGGCTCGAGGGTAGGGTTGAGAGGGATTAGTAG-3')
sequences to amplify the 1.1kb 3' arm of the targeting vector. Their locations are indicated in Figure S7. The six underlined nucleotides in p1 and p4 sequences were converted into AccI and XhoI recognition sequences, GTCGAC and CTCGAG, respectively, to generate each primers. The amplified products were digested by each restriction enzyme: AccI and XhoI for the 2.5 kb 5' arm and SpeI and NotI for the 1.1kb 3' arm, respectively. To construct the targeting vector, the 5' 2.5kb and 3' 1.1kb arms were inserted into the AccI/NotI sites and NheI/XhoI sites of 5' and 3' cloning sites, respectively, of the LacZ/Neo-DTA vector. To generate podocyte specific knockout mice the well established *hNPHS2-Cre* allele was intercrossed to *Epb41l5* conditional mice (provided by Lawrence Holzman - Renal, Electrolyte and Hypertension Division, University of Pennsylvania School of Medicine Philadelphia, PA, USA). As an inducible podocyte specific mouse line we made use of a mouse line expressing a *rtTA* cassette under control of the *hNPHS2* promotor (1). Induction of the respective inducible mouse models was performed according to following protocol: animals at the age of 4 weeks received doxycycline hydrochloride (Fagron) via the drinking water (2mg/ml with 5% (wt/vol) sucrose, protected from light) for a periode of 14 days. For isolation of primary podocytes conditional *Epb41l5* knockout animals were crossed to *Gt(ROSA)26Sor*$^{tm4(ACTB-tdTomato,-EGFP)Luo/J}$ (purchased from JAX mice). Mice were maintained on a SV129 background. All mouse experiments were performed according to the National Institutes of Health Guide for the Care and Use of Laboratory Animals, as well as the German law governing the welfare of

animals. All studies were approved by the Regierungspräsidium Freiburg (G-10/39), Germany.

Urine analyses

Urine was collected at indicated time points and urinary albumin and creatinine were measured using Microflural™ Microalbumin Test (Progen, Heidelberg, Germany) and an Creatinine Kit (Labor+Technik, LT-Sys, Berlin, Germany) according to the manufacturer´s protocol. Proteinuria was expressed as albumin to creatinine ratio (ACR ratio: albumin mg to creatinine mg).

In situ hybridization

Whole mRNA extracts from P1 mouse kidneys served as template for RT-PCR and subsequent cloning of fragments of the coding sequence and 3′-untranslated region. For generating insitu probes against *mEpb41l5* the following primers were used:
mEpb41l Transcript variant 1+2(fp): 5´- AGT TCA GGT TTG TGC CCA TC -3´
mEpb41l Transcript variant 1+2(rp): 5´ - CGG GAT CCT AGT CGA ATG AA -3´
PCR products were cloned into pBluescript II KS (-), linearized and transcribed with T3 and T7 RNA polymerases (Promega, Mannheim, Germany) to generate sense and antisense digoxigenin-labeled probes (digoxigenin RNA labeling mix; Roche Applied Science, Mannheim, Germany). Kidneys at postnatal day 2 were fixed overnight at 4 °C in 4% paraformaldehyde, embedded in paraffin, and sectioned at 8 µm. For mRNA detection, slides were treated with proteinase K, refixed with 4% paraformaldehyde, acetylated by using acetic anhydride (0,25% acetic anhydride in 0,1M triethanolamine (T-1377; Sigma, Schnelldorf, Germany) and hybridized at 68 °C in hybridization buffer (50% formamide, 5× SSC, yeast RNA (50g/ml), 1% SDS, heparin (50g/ml), 0,1% probe). Stringency washes were performed with wash I (50% formamide, 5× SSC (pH4,5), 1%SDS) and wash II (50% formamide, 2× SSC). For detection, slides were incubated with alkaline phosphatase-conjugated anti-digoxigenin antibody 1:3000 at 4 °C overnight followed by BM purple staining (Roche Applied Science, Mannheim, Germany). Digital photographs were captured on an Axioplan2 microscope (Zeiss, Oberkochen, Germany).

SEM and TEM procedures

For scanning electron microscopy kidney samples were fixed in glutaraldehyde and dehydrated by graded ethanol series (70% ethanol, 80% ethanol, 90% ethanol and

100% ethanol), followed by incubation in 50:50 ethanol/Hexamethyldisilazane (Sigma, Schnelldorf, Germany). After incubation in 100% HMDS the solvent was allowed to evaporate. Samples were coated with Gold (Zeiss Semco Nanolab7, Polaron Cool Sputter Coater E 5100, Balzer Cpd 020) and imaged using a Leo 1450 VP scanning electron microscope. Samples for immunogold electron microscopy were fixed and subsequently embedded in Lowicryl K4M resin (Electron Microscopy Sciences). Ultrathin sections were cut and stained by indirect immunogold protocol as described before (for antibodies see supporting information antibodies list)(2).

Immunofluorescence staining of kidney sections

Kidneys were frozen in OCT compound medium immediately after dissection. 4µm sections were cut on a Leica Cryotome. Sections were subsequently fixed in 4% paraformaldehyde, blocked in PBS with 5% BSA and incubated with primary antibodies for 1h or overnight. Sections were washed for several times, then fluorophore-conjugated secondary antibodies (dilution 1:500 - Invitrogen, Karlsruhe, Germany) were applied and incubated for 45 minutes. Human kidney biopsy samples underwent an antigen retrieval step (pH citrate 6.0), and were subsequently processed as outlined above. Imaging was performed either on a Zeiss Axioscope 40FL microscope, equipped with an Axiocam MRc5 digital video camera and conventional HBO lamp (Carl Zeiss, Oberkochen, Germany) or on a LSM510 confocal microscope (Zeiss). Use of human kidney biopsy material was approved by the Scientific-Ethical Committee of the University Medical Center of Freiburg. Control kidney samples were from unaffected areas of tumor nephrectomies. Imaging was performed on a Zeiss Axioscope 40FL microscope, equipped with an Axiocam MRc5 digital video camera and conventional HBO lamp (Carl Zeiss, Oberkochen, Germany).

mRNA expression analysis of human kidney disease entities (NEPHROSEQ)

For analysis of differential mRNA expression levels in human glomerular disease entities the opensource database NEPHROSEQ was used (www.nephroseq.org). For detailed patient information and statistical data see dataset S3.

Antibodies

All antibodies used in this study are collectively described in the SI Materials and Methods (at the end of the SI appendix).

STORM – super resolution microscopy

Briefly, primary antibody diluted in 3% BSA-PBS was applied on the sections and incubated overnight at 4°C. The next day, sections were washed for 30 minutes with PBS at room temperature and then incubated with the STORM-specific secondary antibodies diluted in 3% BSA-PBS at room temperature for 2 hours. STORM image acquisition was performed using a custom-made setup as described (22). Approximately 10,000 images per channel were captured and analyzed using custom software. Further details are provided in the supplemental section. After washing the samples for 30 minutes with PBS at room temperature, immunolabeled sections were postfixed using 3% PFA and 0.1% glutaraldehyde (Electron Microscopy Sciences) in PBS and prepared for STORM imaging. The secondary antibodies were custom conjugated to Alexa647 reporter dye and either Alexa405 or Cy3 activator dyes. Coverglass with the sections on it was inverted onto a slide containing a drop of imaging buffer containing mercaptoethylamine along with an oxygen scavenger system, and coverglass edges were sealed with nail polish.

MS-procedures: Cell lysis and carbamidomethylation

Approximately 1.3 to 2.7 million GFP+ (podocytes) and RFP+ (non-podocytes) cells per individual preparation were used. Each preparation consisted of 4 individual animals, which were pooled after cell sorting. The whole analysis was performed with 4 individual and independent preparations. Snap frozen cell pellets were lysed in 50 mM Tris-HCl, pH 7.8 buffer containing 150 mM NaCl, 1% SDS and complete mini EDTA-free (Roche Diagnostics). Subsequently, 1 µL of benzonase (25 U/µL) and 2 mM $MgCl_2$ were added to the lysates and incubated at 37°C for 30 min. Samples were centrifuged at 4°C and 18,000 *g* for 30 min. Protein concentration of the supernatant was determined by BCA assay according to the manufacturer's protocol (Pierce, Thermo Scientific). Cysteines were reduced with 10 mM dithiothreitol at 56°C for 30 min followed by alkylation of free thiol groups with 30 mM iodoacetamide at room temperature (RT) in the dark for 30 min.

MS-procedures: Sample preparation and proteolysis

Samples for LC-MS analysis were prepared using filter aided sample preparation (FASP) (3, 4) with minor changes. Cell lysates corresponding to 50 µg of protein

were diluted with freshly prepared 8 M urea/100 mM Tris-HCl, pH 8.5 buffer (5). Diluted samples were placed on the Microcon centrifugal devices (30 KDa cutoff) and were centrifuged at 13,500 *g* at RT for 25 min. All the following centrifugation steps were performed under similar conditions i.e. 13,500 *g*, RT, 15 min. To eliminate residual SDS, three washing steps were carried out using 100 µL of 8 M urea/100 mM Tris-HCl, pH 8.5 buffer and finally for the buffer exchange, the devices were washed thrice with 100 µL of 50 mM triethylammonium bicarbonate (TEAB) buffer, pH 8.5. To the concentrated proteins, 100 µL of proteolysis buffer comprising sequencing grade modified trypsin (Promega) 1:25 w/w (enzyme to protein), 0.2 M GuHCl, 2 mM $CaCl_2$ in 50 mM TEAB buffer, pH 8.5 were added and incubated at 37°C for 14 h. The generated tryptic peptides were recovered by centrifugation with 50 µL of 50 mM TEAB buffer, pH 8.5 followed by 50 µL of ultra-pure water. Finally, the peptides were acidified (pH < 3.0) with trifluoroacetic acid (TFA) and the digests were quality controlled as described previously (6). Acidified peptides were completely dried under vacuum (SpeedVac), resolubilized in 0.5 M TEAB (pH 8.5) and the peptide concentration was determined using a NanoDrop 2000 UV-Vis spectrophotometer (Thermo Scientific). ,

MS-procedures: iTRAQ 8-plex labeling and reversed phase fractionation at pH 6.0

Prior to labeling with iTRAQ reagents, each sample (~ 0.5 µg) was analyzed on a LC-MS system. The sample amounts were corrected based on the comparison of total ion chromatograms (TICs) to compensate for the systematic errors such that each sample had identical starting material before labeling. After adjustment, 25 µg of tryptic peptides of each sample were labeled with iTRAQ 8-plex reagents (AB Sciex) according to the manufacturer's instructions. After incubation, the samples were pooled and the reaction was quenched by adding 100 µL of ultra-pure water. The multiplexed sample was concentrated to ~20 µL under vacuum and subsequently acidified with TFA (1% final concentration). Sample cleanup was done with a C18 SPE cartridge (15 mg, Varian) using a vacuum manifold system and the eluted peptides were dried in a SpeedVac. The dried multiplexed sample was resolubilized in buffer A (10 mM ammonium acetate, 0.4 mM formic acid (FA), pH 6.0) and 50 µg were fractionated by reversed phase chromatography at pH 6.0 on an Zorbax 300SB-C18 column, 1 x 150 mm, 5 µm particle size column (Agilent) using an UltiMate 3000

HPLC (Thermo Scientific) using a binary buffer system; buffer A: 10 mM ammonium acetate, 0.4 mM FA, pH 6.0 and buffer B: 84% acetonitrile (ACN) in 10 mM ammonium acetate, 0.4 mM FA, pH 6.0. Peptides were loaded onto the column with buffer A at a flowrate of 12.5 µL/min and separation was carried out using the following gradient: 0-3% B in 10 min, 3-50% B in 65 min, 50-60% B in 5 min, 60-95% B in 5 min, 95% B hold for 5 min, 95%-3% B in 5 min and finally re-equilibrate the column with 3% B for 20 min. In total, 24 fractions were collected at 30 sec intervals from min 15 to 70 in a concatenation mode.

LC-MS/MS analysis

Each fraction was resolubilized in 45 µL of 0.1% TFA and 1/3rd of each sample was analyzed by nano-LC-MS/MS using an Ultimate 3000 nano RSLC system coupled to a Q Exactive mass spectrometer (both Thermo Scientific). Peptides were preconcentrated on a 75 µm x 2 cm C18 trapping column for 10 min using 0.1% TFA with a flow rate of 20 µL/min followed by separation on a 75 µm x 50 cm C18 main column (both Pepmap, Thermo Scientific) with a 127 min LC gradient ranging from 3-42% of B (84% ACN in 0.1% FA) at a flow rate of 250 nL/min. The Q Exactive was operated in data-dependent acquisition mode and MS survey scans were acquired from m/z 300 to 1,500 at a resolution of 70,000 using the polysiloxane ion at m/z 371.101236 as lock mass (7). Precursor isolation window was set as 2.0 m/z and the fifteen (Top15) most intense signals were subjected to higher energy collision dissociation (HCD) with a normalized collision energy of 35% at a resolution of 17,500 taking into account a dynamic exclusion of 12 s. Automated gain control (AGC) target values and fill times were set to $3x10^6$ and 120 ms for MS and $1x10^6$ and 250 ms for MS/MS, respectively with an underfill ratio of 10%. For charge state reduction, a 10% (v/v) NH_4OH solution was placed at the nano-ESI source as previously described (8).

Protein enrichment and functional annotation analysis

Detected proteins (iTRAQ podocyte proteome) were identified as enriched/upregulated with a “log2 ratio podocytes/non-podocytes” >0.5 or as non-upregulated with a log2 ratio <0.5. Gene ontology term (GO-Term) annotation was implemented using the UniProt and MGI database (9, 10). The GO-Term: “GO:0005925 focal adhesion” (MGI database) was used to generate a list of

podocyte enriched focal adhesion proteins. These focal adhesion proteins were assembled to functional groups as previously described by Kuo JC et al. (11). To generate a network out of these proteins, the list of focal adhesion proteins found as enriched was imported into Cytoscape (version 3.2.1) (12). Protein-protein interactions were added by merging this network with a human interactome from the BioGRID (release 3.2.105) database (13). Protein and interaction duplications were removed. In order to generate an unbiased list of potential podocyte specific focal adhesion proteins, a merged focal adhesion proteome from Horton ER et al. was merged with the list of proteins enriched in podoyctes (14). This candidate list was subsequently filtered for protein domains enriched in focal adhesion proteins. This list of protein domains enriched in focal adhesion proteins was generated by analysis of the consensus integrin adhesome from Horton et al. (14) Go-Term and InterPro protein domain enrichment analysis was done using the FunRich (version 2.1.2) functional enrichment analysis software (15, 16). The mice proteome database from UniProt was chosen as a background database. For enriched Go-Terms hypergeometric uncorrected p-values are shown on the charts (Figure S2). Also Benjamini-Hochberg corrected FDR values led to significant p-values for these Go-Terms.

Isolation of focal adhesion complexes

A technique for isolation of focal adhesion complexes was described previously (11, 14). This technique was combined with a SILAC based quantitative MS approach (17). In brief, human immortalized podocytes were SILAC labeled under growth conditions at 33°C. After 14 days, podocytes were seeded to a 50µg/ml collagen IV coated 15cm cell culture dish and were cultured for 24 hours. For stabilization and linkage of focal adhesion complexes to the underlying ECM cells were incubated with two protein cross-linkers (DSP (3,3'-Dithiobis(sulfosuccinimidylpropionate); 100mM; Sigma-Aldrich) and DPPB (1,4-Bis[3-(2-pyridyldithio)propionamido]butane; 10mM; Sigma-Aldrich)) for 10 minutes. Cross-likers were removed by washing with PBS and quenched with 1M Tris-HCl (pH 7,5, 10 min). After additional washing in PBS, cell bodies were removed via cell lysis using RIPA buffer (25mM Tris-HCL, 150mM NaCl , 1% Triton-X-100, 0,2% SDS +0,5% Sodium Deoxycholic acid, pH7,5, containing proteinase inhibitors) for 3 minutes at 4°C followed by application of hydrodynamic force using a waterpik (washing 2x10s with PBS). ECM linked focal adhesion

complexes were now isolated by scraping in scraping buffer (100mM Tris-HCl (pH 7,6), 4% (w/v) SDS). Total protein concentrations were measured and samples were balanced. Laemmli buffer (with DTT) was added and focal adhesion complexes were denatured at 70°C for 10 min. MS analysis and Western blotting was performed subsequently. Data processing and annotation of external databases was performed as described above. A core focal adhesome was defined by merging the consensus integrin adhesome (14) with a literature curated adhesome(18). EPB41L5 dependent regulated components of this core adhesome were graphically shown in Figure 7. For further information see also dataset S2.

Isolation of primary podocytes for *in vitro* experiments

Kidneys were cut in small pieces and mixed in 3ml (per kidney pair) prewarmed digestion solution (digestion solution containing 1mg/ml Collagenase, 1mg/ml Proteinase, 50U/ml DNase in 1xHBSS). The solution was resuspended and incubated at 37°C for 7min. After incubation the solution was put on a cell strainer and it was rubbed through the cell strainer using the stamp of a 5ml syringe. The strainer was washed using ice cold 1xHBSS. The flow-through was filtered through a cell strainer and washed again with 1xHBSS. Glomeruli were washed from this cell strainer using 1xHBSS and collected. The obtained glomeruli were centrifuged at 4°C, 2000g for 10min, the supernatant was removed and the glomeruli pellet was dissolved in primary podocyte medium (RPMI medium supplemented with 10% FBS, Penicillin/Streptomycin, ITS). Cell culture flask were coated using Collagen IV dissolved in acetic acid solution and finally the resuspended glomeruli were seeded and cultured at 37°C and 5% $CO_{2.}$. Glomerular cells were grown out for 7 days and FACS sorted to obtain the GFP labeled podocyte fraction.

Crispr/Cas9 mediated knockout of EPB41L5

For the generation of *EPB41L5* knockout in immortalized human podocytes (generous gift from Moin Saleem, Bristol, UK) the Crispr/CAS9 genome editing technology was applied. gRNAs targeting exon 1 of the human *EPB41L5* gene were designed using a web-based platform (e-crisp.org - http://www.e-crisp.org/E-CRISP/) and further subcloned in targeting CRISPR nuclease vectors with an OFP reporter according to manufacturer´s instructions (guideRNA: 5'-GACTTAGAATCTCCAGCTGC(AGG)-3' - gene-art – Invitrogen, Karlsruhe, Germany). After initial validation in mixed cell-populations employing the nuclease

surveyor technology (Integrated DNA technologies, Leuven, Belgium), immortalized human podocytes were electroporated with CAS9 nuclease and respective gRNAs. After 48 hours, OFP positive cells were selected via FACS and single cell clones were further grown to subsequent mutation analysis. DNA of respective single cell clones was isolated and further PCR amplified and homozygous mutated clones were preselected applying a restriction enzyme digest with PstI (5'-CTGCA/G-3' New England BioLabs, Ipswich, MA, USA). These clones were subcloned and analyzed using Sanger Sequencing (primer pairs for amplification – E1 fw 5´-TCTTGAACTCCTGGCTCTA-3´; E1 rev 5´-TTTGGAGCTCAGCAAGACCT-3´). Only clones with homozygous mutations resulting in premature stop-codons were selected for further analysis. Loss of protein was furthermore confirmed using western blot.

Single cell migration assay

Cells were seeded on ibidi µ-treat dishes (ibidi, Martinsried, Germany) and cultivated in standard medium (see above). Observation of single cell migration was performed using a Nikon Biosstation IM device (Nikon, Düsseldorf, Germany). Primary podocytes were identified by *NPHS2Cre* driven podocyte specific GFP expression and phase contrast observation was performed for 12 hours. In the case of immortalized podocytes imaging was only performed using phase contrast. Further analysis was done by using the ManualTracking and ChemoTaxis plugin for NIH ImageJ 1.46.

Adhesion, cellular spreading assays and analysis of focal adhesion morphology

Adhesion assays on collagen IV coated surfaces were performed as previously described (19). In brief, cells were trypsinized, counted with an automated cell counting tool (Biorad, Munich, Germany) and equal amounts of cells (40.000 cells per genotype and technical replicate) were seed for 15 minutes on 50µg/ml collagen IV precoated 96 well plates. After standardized washing procedures, crystal violet was applied and OD as a measure of adhered cells was quantified on a photometer (TECAN, Crailsheim, Germany). For cell spreading assays equal amounts of cells were seeded on pre-coated cover-slips or ibidi 8-well dishes (if not statet otherwise precoating was performed with 50µg/ml collagen IV or fibronectin respectively, for spreading under titrated ECM concentrations 0.5µg/ml, 10µg/ml and 50µg/ml were applied for either collagen IV or fibronectin; fibronectin from BD Biosciences and

collagen IV from Sigma) for indicated time points. After brief fixation in PFA 4%, cells were stained with Phalloidin and imaged using an Axioscope 40FL microscope setup 20x magnification. Randomly chosen images were captured and analyzed using ImageJ NIH. Following binarization of images individual cell areas were measured. Circularity analysis was also performed using implemented function of ImageJ NIH. For the quantification of focal adhesion fractions cells were seeded for 30 and 45 minutes, fixed and stained. Individual cells were assessed for 3 criteria (a: only edge-staining; b: nascent adhesions; c: maturated adhesions). Focal adhesion morphology was assessed by staining for the focal adhesion component PAXILLIN. Image acquisition was performed using a Zeiss Axioscope 40FL microscope, equipped with a 63x objective. Evaluation of focal adhesion size and distribution was performed with a custom written macro embedded in FIJI NIH ImageJ 1.46. For the quantification of cellular protrusions cells were seeded for 30 minutes at 20µg/ml collagen IV coated glass cover slips, fixed and stained. Protrusions of individual cells were counted and analyzed. To assess major:minor axis ratios individual cells were analyzed using NIH ImageJ 1.46. Analysis of fluorescence intensities across the cell border were performed using the line scan function of FIJI NIH ImageJ 1.46. At least 10 representative cells per condition were measured and at least 3 biological replicates were analyzed. For treatment and washout experiments equal amounts of cells were seeded for 4 hours on collagen IV or fibronectin pre-coated glass cover-slips. Then treatment of cells using the myosin-II inhibitor blebbistatin (Sigma, Schnelldorf, Germany) and the ROCK inhibitor Y-27362 (Sigma) were performed as indicated in the individual experiments, for 40 minutes. Treatment of cells using doxorubicin and protramine sulfate (Sigma) were performed as indicated in the individual experiments. For spreading experiments under doxorubicin or protramine sulfate treatment, cells were pre-treated with 2µg/ml doxorubicin for 24 hours or 300µg/ml protamine sulfate for 10 minutes.

Live cell imaging

For analysis of pseudopod dynamics immortalized human podocytes were transfected with RFP-tagged versions of Lifeact via electroporation. After 24 hours cells were seeded on ibidi dishes (ibidi, Martinsried, Germany) and recorded on a Zeiss Cell Observer equipped with a LCI Plan-Neofluoar 63x/1.3 objective and Tokai Heat Incubator (controlled heating, controlled CO2 atmosphere). Respective imaging

sequences were analyzed using Image J NIH Version 1.47. Protrusion rate generation was calculated by counting every newly generated protrusion in a 10 minute time frame.

siRNA knockdown in immortalized human podocytes

Generation of siRNA mediated knockdown of *ARHGEF18* in immortalized human podocytes was performed using previously published siRNA sequences (siRNA p114Rhogef I - 5′-UCAGGCGCUUGAAAGAUA-3′; p114Rhogef II - 5′-GGACGCAACUCGGACCAAU-3′ (20)). Transfection was performed using Amaxa nucleofector technology (Lonza, Basel, Switzerland) according to manufacturer´s instructions. Efficiency of the knockdown was cofirmed 48 and 72 hours after transfection using western blot. Spreading experiments were performed and quantified as described above.

Analysis of activated RhoA and Rac1 levels using G-LISA

Cells were serum starved for 3 consecutive days at 1% FCS in standard RPMI1640 medium. After completion of the starvation period, cells were trypsinized and equal amounts were seeded on either collagen IV or fibronectin coated 10 cm dishes for either 20 or 45 minutes. Dishes were washed with ice-cold PBS buffer twice and lysis was performed at 4°. Lysates were equalized due to protein content and analyzed according to the manufacturers instruction (RhoA G-LISA activation assay kit – BK124; Rac1,2,3 G-LISA activation assay kit – BK125, Cytoskeleton, USA).

Immunoprecipitation and pulldown

Co-immunoprecipitation was performed as described previously (21). Briefly, HEK 293T cells were transiently transfected with 4µg DNA of the indicated constructs using the PEI (Polyethylenimin) method. After incubation for 24 h, the cells were lysed in 1% Triton X-100 lysis buffer (1% Triton X-100, 20ml Tris-HCL, 50mM NaCL, 50mM NaF, 15mM $Na_4P_2O_7$, 1mM EDTA, pH 7.4) (30 min; 4°C). Cell lysates were incubated with mouse anti-V5-tag antibody, rabbit ant-VSV-tag antibody, rabbit anti-ARHGEF18 antibody or anti-Flag M2 agarose affinity beads (Sigma Aldrich) for 1 h at 4°C. Thereafter lysates were incubated with 20 µl of protein G-Sepharose beads for mouse antibodies and with 20 µl of protein A-Sepharose beads for rabbit antibodies for 0,5 - 1 h at 4°C. Recombinant GST tagged protein was produced in a BL21(DE3)

E. coli strain. The transformation, expression and purification were performed according to standard procedures (22). GST tagged protein was pre-bound to 25µl glutathione-Sepharose beads (GE Healthcare) and subsequently incubated with lysates of human immortalized podocytes or VSV-ARHGEF18 overexpressing HEK293T cells for 1 hour at 4°. The beads were washed 5 times with lysis buffer, and bound proteins were resolved in *Laemmli sample buffer* (95°C, 5 min). Precipitated proteins were separated by standard SDS-polyacrylamide gel electrophoresis. Following constructs were used: N or C-terminal tagged constructs (either FLAG or GFP tag) for human EPB41L5 were purchased and used according to manufacturer´s instructions (Genescript, New Jersey, USA). VSV-tagged *ARHGEF18* was generously provided by K. Matter (20). N-terminal V5-, FLAG-, GFP-tagged constructs of full length and truncated EPB41L5 were created by cloning into pcDNA6 vector using standard cloning procedures. N-terminal GST-tagged constructs were created by cloning into pGEX-4T-3 vector.

Expression of *EPB41L5* constructs in immortalized human podocytes

For transfection of immortalized human podocyte cells (kindly provided by M. Saleem, University of Bristol, UK) electroporation as described above was performed. N or C-terminal tagged constructs (either FLAG or GFP tag) for human EPB41L5 were purchased and used according to manufacturer´s instructions (Genescript, New Jersey, USA). Rescue experiment in respective EPB41L5 KO cells were performed by re-expression of GFP-tagged versions of human EPB41L5 as outlined above (either full length or respective truncations). Cell size area, as well as pseudopod formation and p-MLC fluorescence intensity was recorded as indicated above and knockout cells expressing only GFP served as controls (for analysis only cells with equalized expression levels were selected).

Supplemental References

1. Shigehara T*, et al.* (2003) Inducible podocyte-specific gene expression in transgenic mice. *Journal of the American Society of Nephrology : JASN* 14(8):1998-2003.
2. Horvat R, Hovorka A, Dekan G, Poczewski H, & Kerjaschki D (1986) Endothelial cell membranes contain podocalyxin--the major sialoprotein of visceral glomerular epithelial cells. *The Journal of cell biology* 102(2):484-491.
3. Manza LL, Stamer SL, Ham A-JL, Codreanu SG, & Liebler DC (2005) Sample preparation and digestion for proteomic analyses using spin filters. *PROTEOMICS* 5(7):1742-1745.
4. Wisniewski JR, Zougman A, Nagaraj N, & Mann M (2009) Universal sample preparation method for proteome analysis. *Nat Meth* 6(5):359-362.
5. Kollipara L & Zahedi RP (2013) Protein carbamylation: In vivo modification or in vitro artefact? *PROTEOMICS* 13(6):941-944.
6. Burkhart JM, Schumbrutzki C, Wortelkamp S, Sickmann A, & Zahedi RP (2012) Systematic and quantitative comparison of digest efficiency and specificity reveals the impact of trypsin quality on MS-based proteomics. *Journal of Proteomics* 75(4):1454-1462.
7. Olsen JV*, et al.* (2005) Parts per Million Mass Accuracy on an Orbitrap Mass Spectrometer via Lock Mass Injection into a C-trap. *Molecular & Cellular Proteomics* 4(12):2010-2021.
8. Thingholm TE, Palmisano G, Kjeldsen F, & Larsen MR (2010) Undesirable Charge-Enhancement of Isobaric Tagged Phosphopeptides Leads to Reduced Identification Efficiency. *Journal of Proteome Research* 9(8):4045-4052.
9. UniProt C (2015) UniProt: a hub for protein information. *Nucleic acids research* 43(Database issue):D204-212.
10. Eppig JT*, et al.* (2015) The Mouse Genome Database (MGD): facilitating mouse as a model for human biology and disease. *Nucleic acids research* 43(Database issue):D726-736.
11. Kuo JC, Han X, Hsiao CT, Yates JR, 3rd, & Waterman CM (2011) Analysis of the myosin-II-responsive focal adhesion proteome reveals a role for beta-Pix in negative regulation of focal adhesion maturation. *Nature cell biology* 13(4):383-393.
12. Shannon P*, et al.* (2003) Cytoscape: a software environment for integrated models of biomolecular interaction networks. *Genome research* 13(11):2498-2504.
13. Chatr-Aryamontri A*, et al.* (2015) The BioGRID interaction database: 2015 update. *Nucleic acids research* 43(Database issue):D470-478.
14. Horton ER*, et al.* (2015) Definition of a consensus integrin adhesome and its dynamics during adhesion complex assembly and disassembly. *Nature cell biology* 17(12):1577-1587.
15. Hunter S*, et al.* (2009) InterPro: the integrative protein signature database. *Nucleic acids research* 37(Database issue):D211-215.
16. Pathan M*, et al.* (2015) FunRich: An open access standalone functional enrichment and interaction network analysis tool. *Proteomics* 15(15):2597-2601.
17. Kuttner V*, et al.* (2013) Global remodelling of cellular microenvironment due to loss of collagen VII. *Molecular systems biology* 9:657.

18. Winograd-Katz SE, Fassler R, Geiger B, & Legate KR (2014) The integrin adhesome: from genes and proteins to human disease. *Nature reviews. Molecular cell biology* 15(4):273-288.
19. Humphries MJ (2009) Cell adhesion assays. *Methods in molecular biology* 522:203-210.
20. Terry SJ*, et al.* (2011) Spatially restricted activation of RhoA signalling at epithelial junctions by p114RhoGEF drives junction formation and morphogenesis. *Nature cell biology* 13(2):159-166.
21. Huber TB*, et al.* (2003) Nephrin and CD2AP associate with phosphoinositide 3-OH kinase and stimulate AKT-dependent signaling. *Molecular and cellular biology* 23(14):4917-4928.
22. Huber TB*, et al.* (2003) The carboxyl terminus of Neph family members binds to the PDZ domain protein zonula occludens-1. *The Journal of biological chemistry* 278(15):13417-13421.

Supporting Information

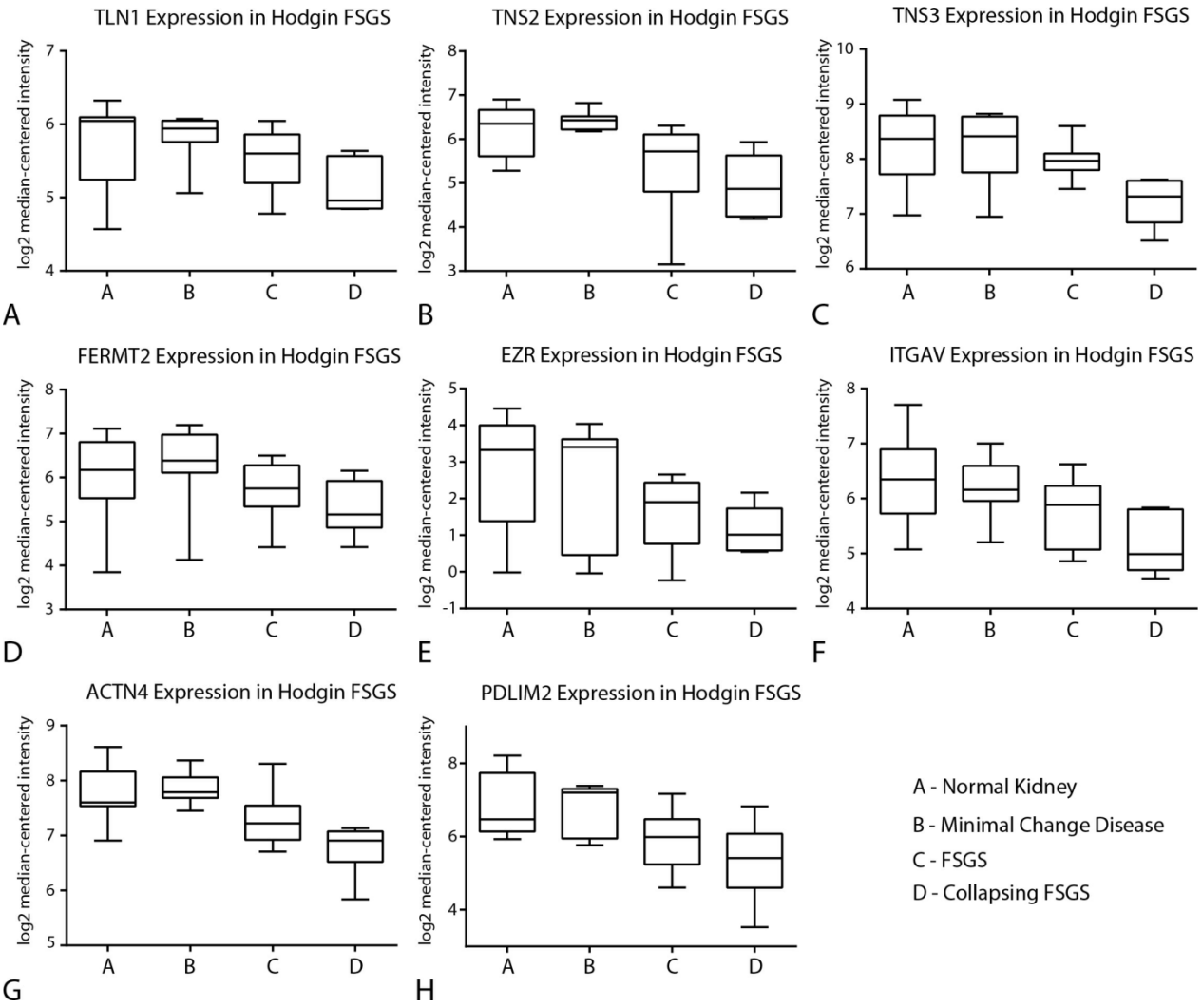

<u>Supplemental Figure 1</u>: Analysis of mRNA expression levels of focal adhesion proteins in human glomerular disease entities

(A-H) Expression values of respective focal adhesion proteins (TALIN-1, TENSIN-2, TENSIN-3, FERMT2, EZRIN, INTEGRIN-alphaV, ACTININ-4, PDLIM2) were analyzed using the open source database NEPHROSEQ. As disease entities minimal change disease, focal segmental sclerosis and collapsing focal segmental glomerular sclerosis were analyzed (for statistical data see dataset S3). All FA proteins showed a diminished expression level in respective disease entities when compared to controls (human nephrectomy samples).

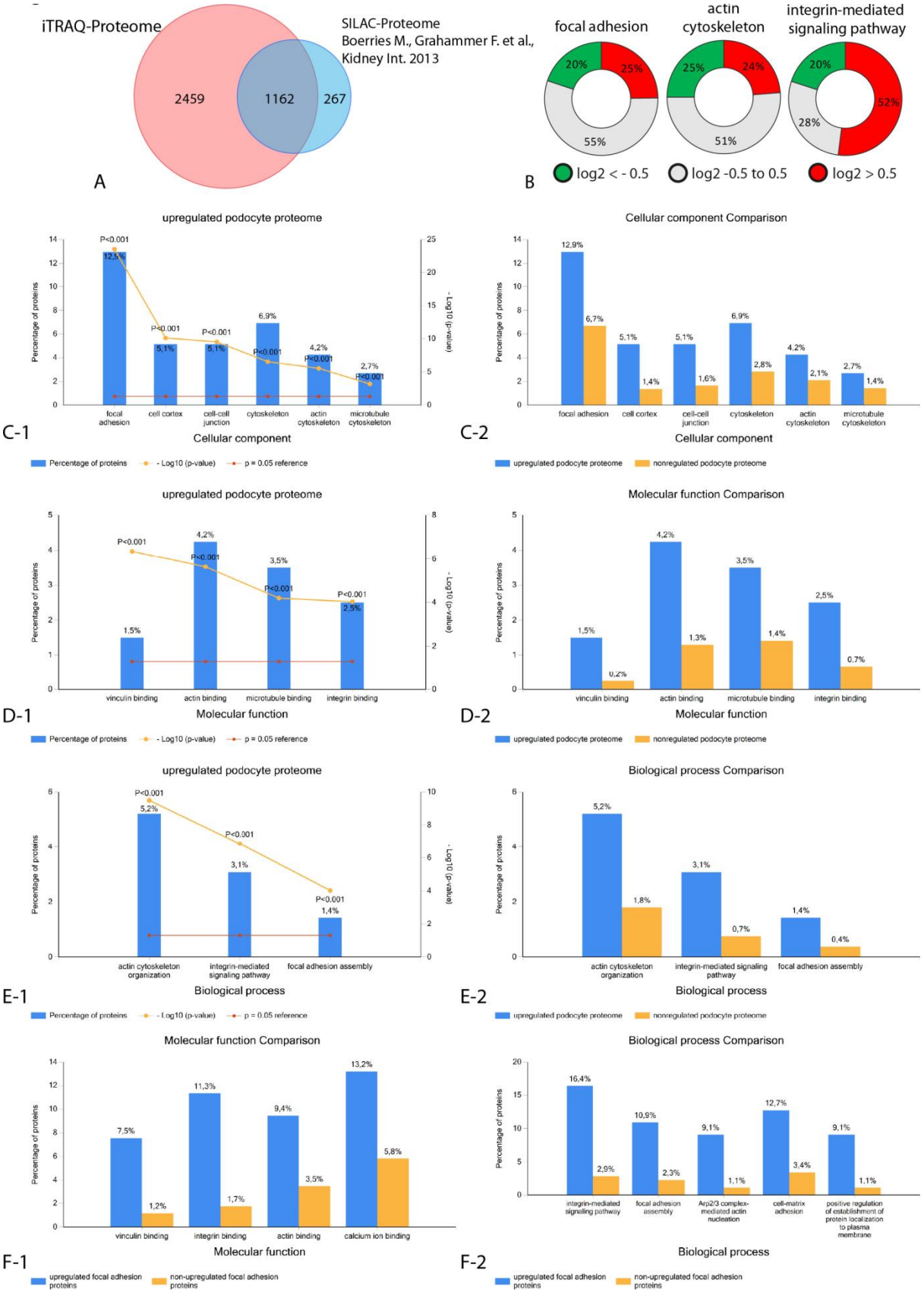

<u>Supplemental Figure 2</u>: Analysis of mapped podocyte adhesome

(A) Venn diagram comparing the coverage of detected proteins between a previous SILAC labeled podocyte proteomics approach [19] and the actual iTRAQ labeled

proteomics approach. **(B)** Sub-analysis of the focal adhesome data set revealed enrichment of integrin-mediated signaling pathways **(C-F)** Analysis of cellular component, molecular function and biological process of respective enriched FA components (see also dataset S1): B1, C1 and D1 GO-Term analysis for log2 fold >0.5 enriched proteins; B2, C2 and D2 GO-Term comparison between log2 fold >0.5 versus log2 fold <0.5 proteins; E1 and E2 selected FA-proteins with log2 fold change >0.5 were analyzed again for GO-term enrichment.

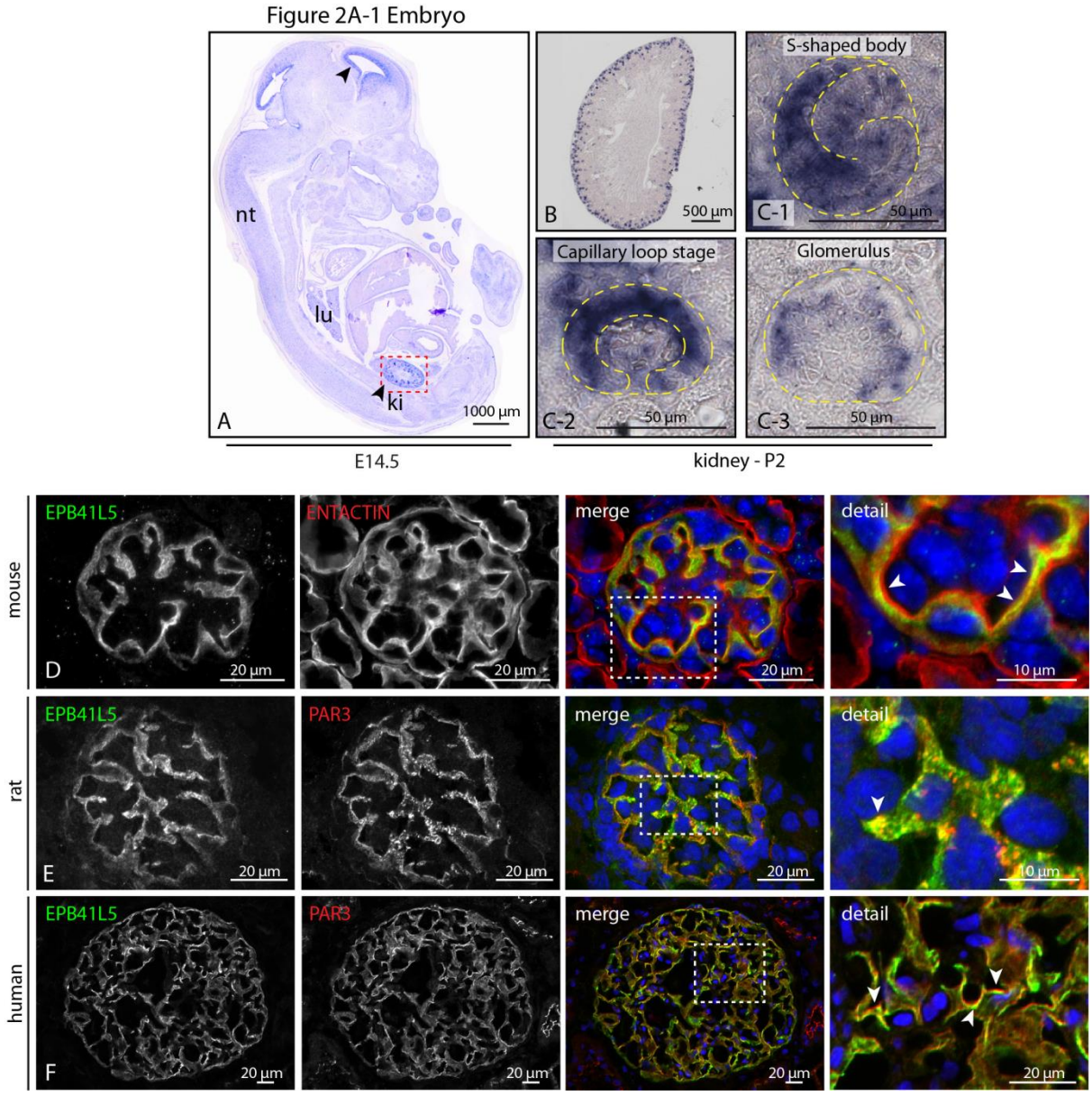

<u>Supplemental Figure 3</u>: Expression of *Epb41l5* in murine development and localization in glomeruli

(A) In situ hybridization on E14.5 murine embryo revealed strongest expression in the kidney (nt= neural tube, lu= lung, ki=kidney; black arrowhead indicates expression in the developing CNS, red boxed area highlights developing kidney). **(B-C)** During glomerular development (C1-C3: comma shaped body, capillary loop stage and glomerulus) *EPB41L5* was specifically detected in podocytes (glomerular structures are highlighted by yellow dotted lines). **(D-F)** Immunofluorescence for EPB41L5 on murine, rat and human glomerular sections (white arrowheads indicate enrichment in the podocyte compartment).

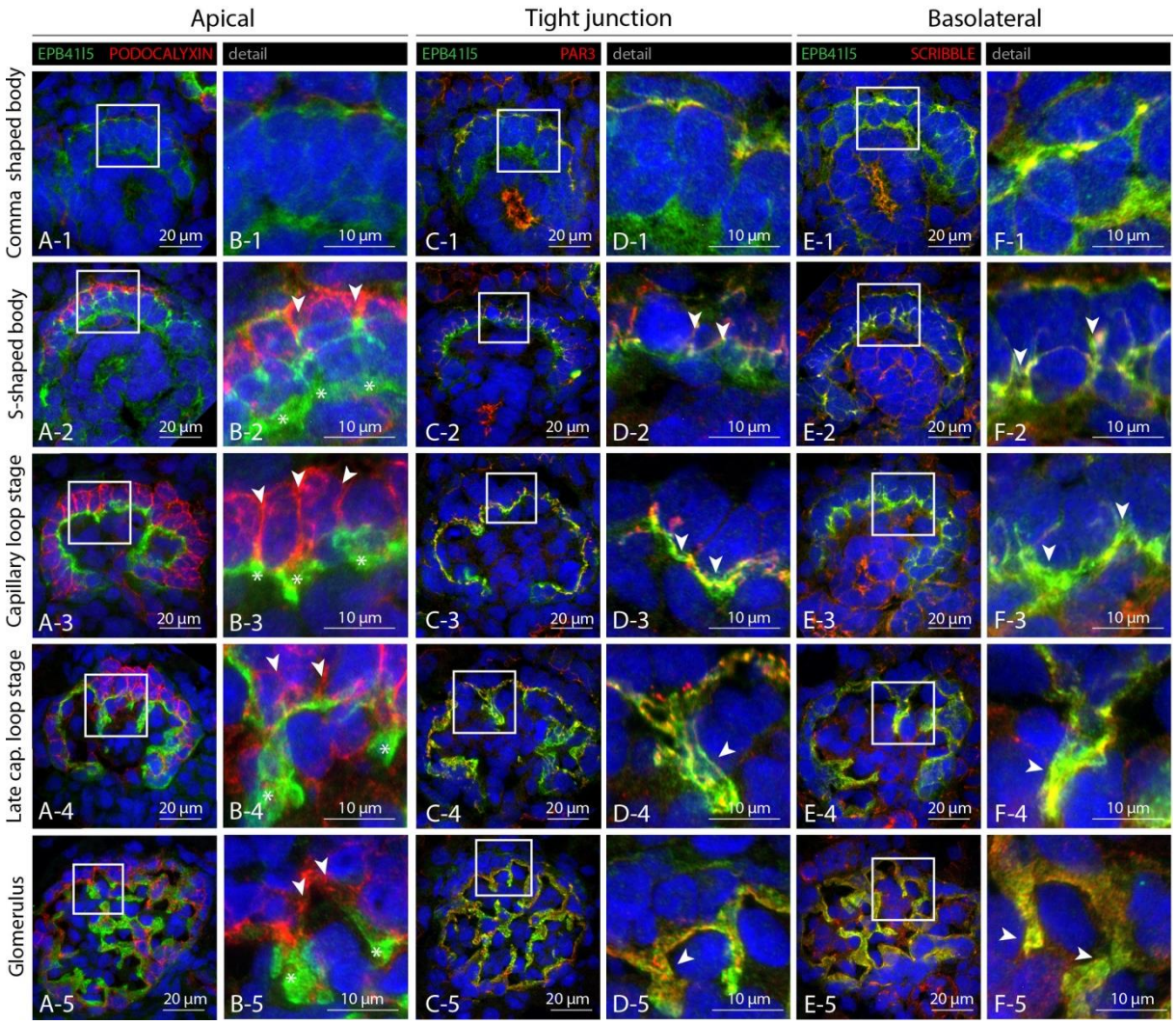

<u>Supplemental Figure 4:</u> Apico-basal polarization of podocytes while glomerular maturation

(A-F) Antibody staining on cryo-sections of P0 murine kidneys: EPB41L5 together with the apical marker PODOCALYXIN showed mutually exclusive staining (B-1-B-5). When EPB41L5 was co-stained together with the tight junction marker PAR3 overlap could be visualized at the comma shaped stage (D-3), but at later stages EPB41l5 located more basal than PAR3(D-4 & D-5). The basolateral marker SCRIBBLE perfectly co-localized with EPB41L5 in every developmental stage of the glomerulus (F-1 – F-5).

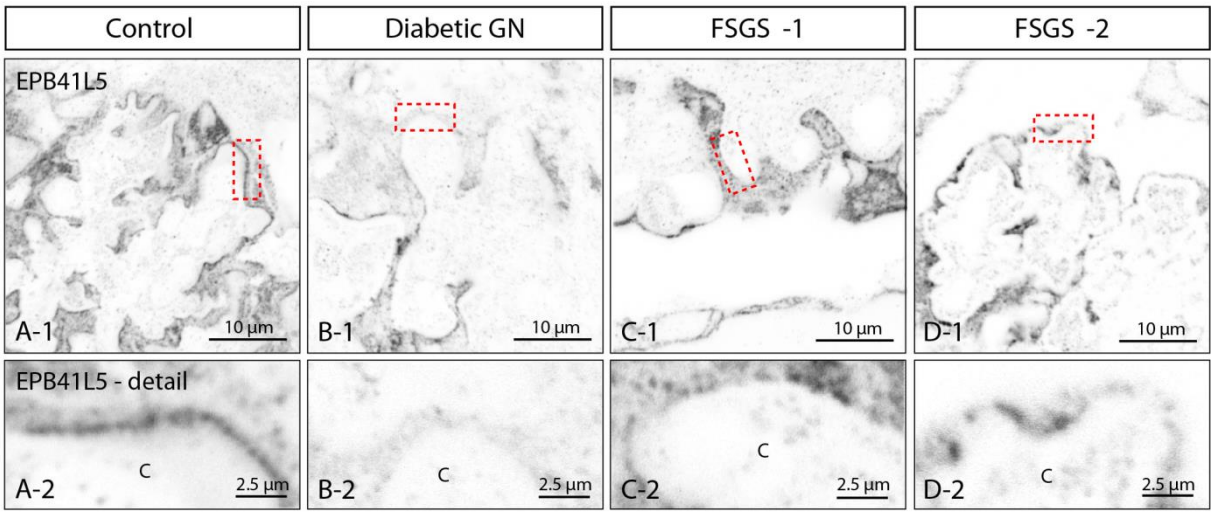
Control
Diabetic GN
FSGS -1
FSGS -2
EPB41L5
A-1
B-1
C-1
D-1
10 µm
EPB41L5 - detail
A-2
B-2
C-2
D-2
C
2.5 µm

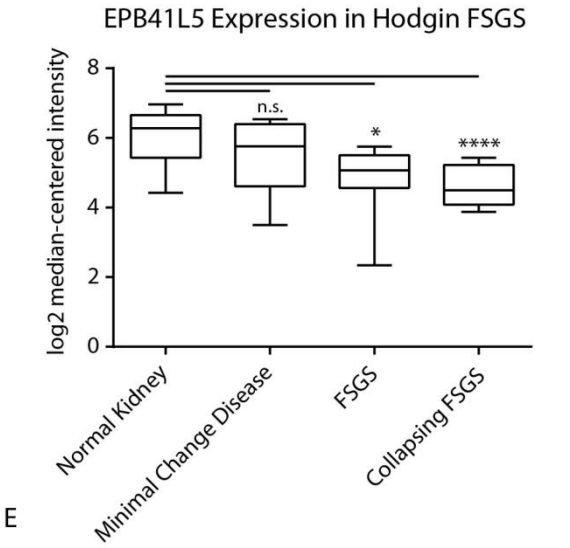
EPB41L5 Expression in Hodgin FSGS
log2 median-centered intensity
n.s.
*
****
Normal Kidney
Minimal Change Disease
FSGS
Collapsing FSGS

E

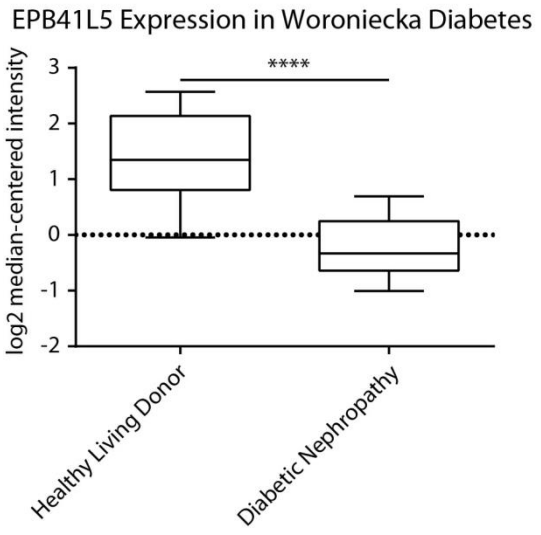
EPB41L5 Expression in Woroniecka Diabetes
log2 median-centered intensity
****
Healthy Living Donor
Diabetic Nephropathy

F

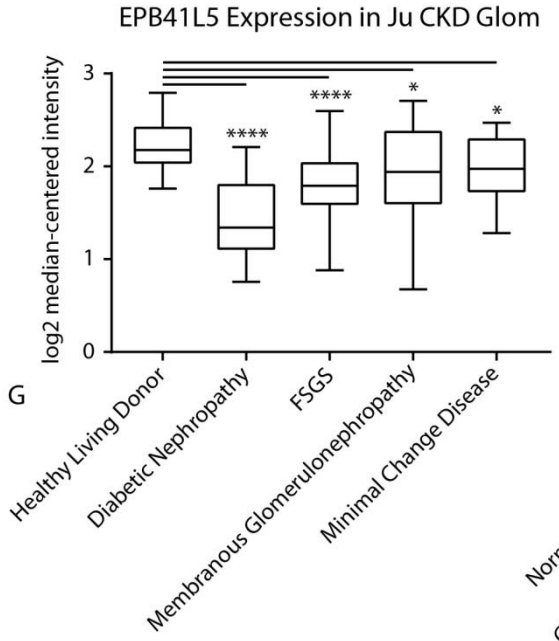
EPB41L5 Expression in Ju CKD Glom
log2 median-centered intensity
****
****
*
*
Healthy Living Donor
Diabetic Nephropathy
FSGS
Membranous Glomerulonephropathy
Minimal Change Disease

G

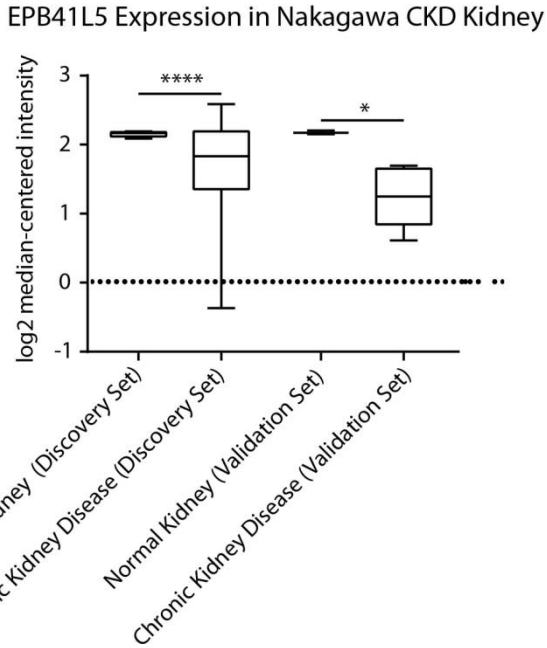
EPB41L5 Expression in Nakagawa CKD Kidney
log2 median-centered intensity
****
*
Normal Kidney (Discovery Set)
Chronic Kidney Disease (Discovery Set)
Normal Kidney (Validation Set)
Chronic Kidney Disease (Validation Set)

H

<u>Supplemental Figure 5:</u> EPB41L5 shows decreased expression levels in human glomerular diseases

(A-D) Immunofluorescence studies on human biopsy samples (Diabetic nephropathy and focal segmental glomerulosclerosis) revealed a diminished and granular signal intensity of EPB41L5, predominantly at the basal compartment of glomerular podocytes (red boxes indicate zoom-in areas). (E-H) Analysis of expression levels for EPB41L5 in different glomerular disease entities shows decreased expression compared to control or healthy donors (for statistical data see dataset S3).

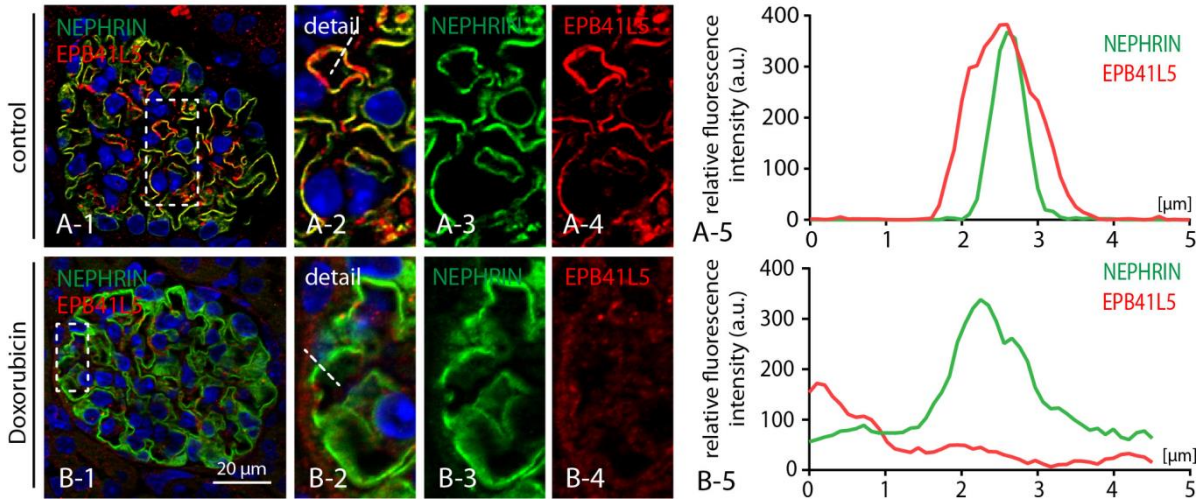

<u>Supplemental Figure 6</u>: EPB41L5 shows altered localization pattern in experimental murine doxorubicin mediated glomerulopathy

(A-B) Immunofluorescence studies of doxorubicin treated animals revealed diminished signal intensity EPB41L5. Respective line scans across the glomerular filtration barrier (white dotted lines) reflect the altered signal intensities for NEPHRIN and EPB41L5.

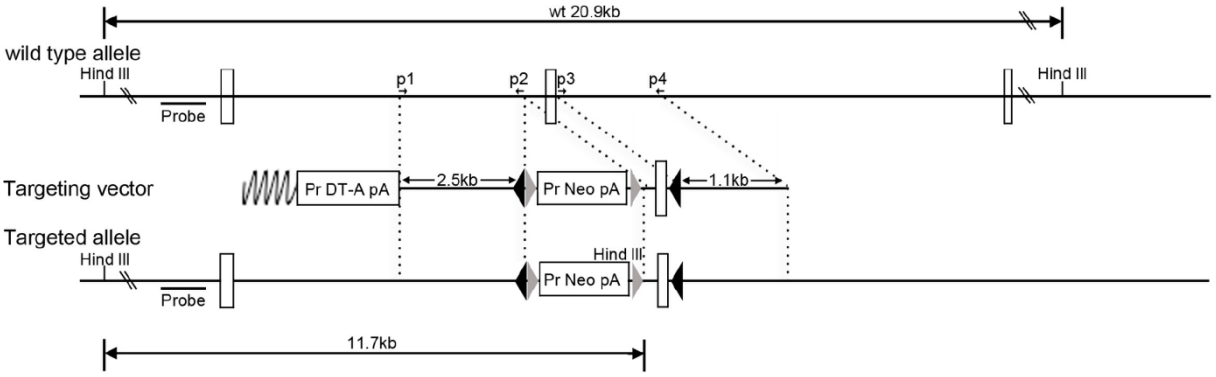

A

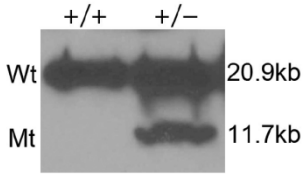

B

<u>Supplemental Figure 7</u>: Targeting strategy and generation of a conditional *Epb41l5* allele

(A) Schematic representation of the wild type *Epb41l5* allele (top), the targeting vector (middle), and the predicted mutant allele (bottom). Black triangles, *loxP* sequence; Gray triangles, *frt* sequences; Neo, neomycine resistant gene; DT-A, diphtheria toxin A-fragment gene. Probe indicates the location of the probe used for Southern blot analysis. **(B)** An example of Southern blot analysis for F1 offspring with the probe indicated in **(A)**.

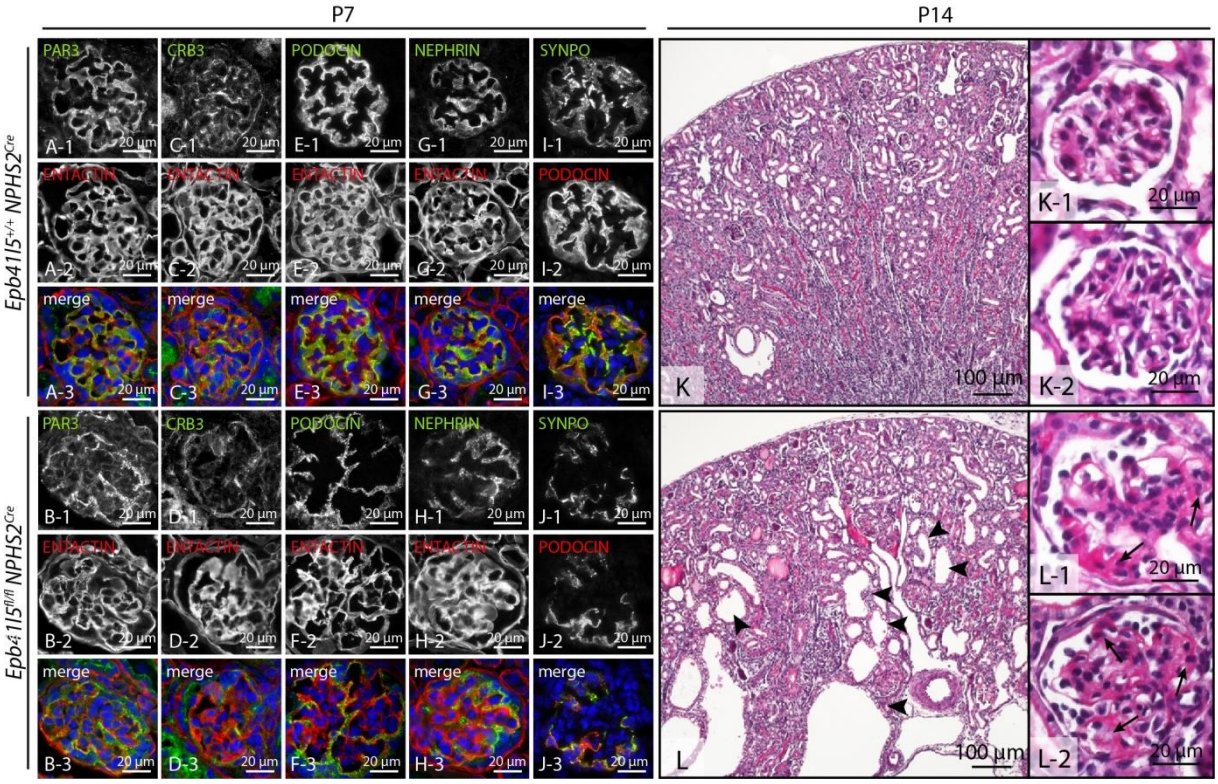

<u>Supplemental Figure 8</u>: Podocyte specific knockout of *Epb41l5* leads to glomerulosclerosis

(A-J) Analysis of podocyte marker proteins showed altered expression and localization patterns in respective *Epb41l5* knockout podocytes compared to wild type animals at P7. **(K-L)** Histological evaluation at P14 demonstrated prominent cystic tubular degeneration (L - black arrowheads) and pronounced glomerulosclerosis (L-1 and L-2; black arrows) in *Epb41l5* knockout animals.

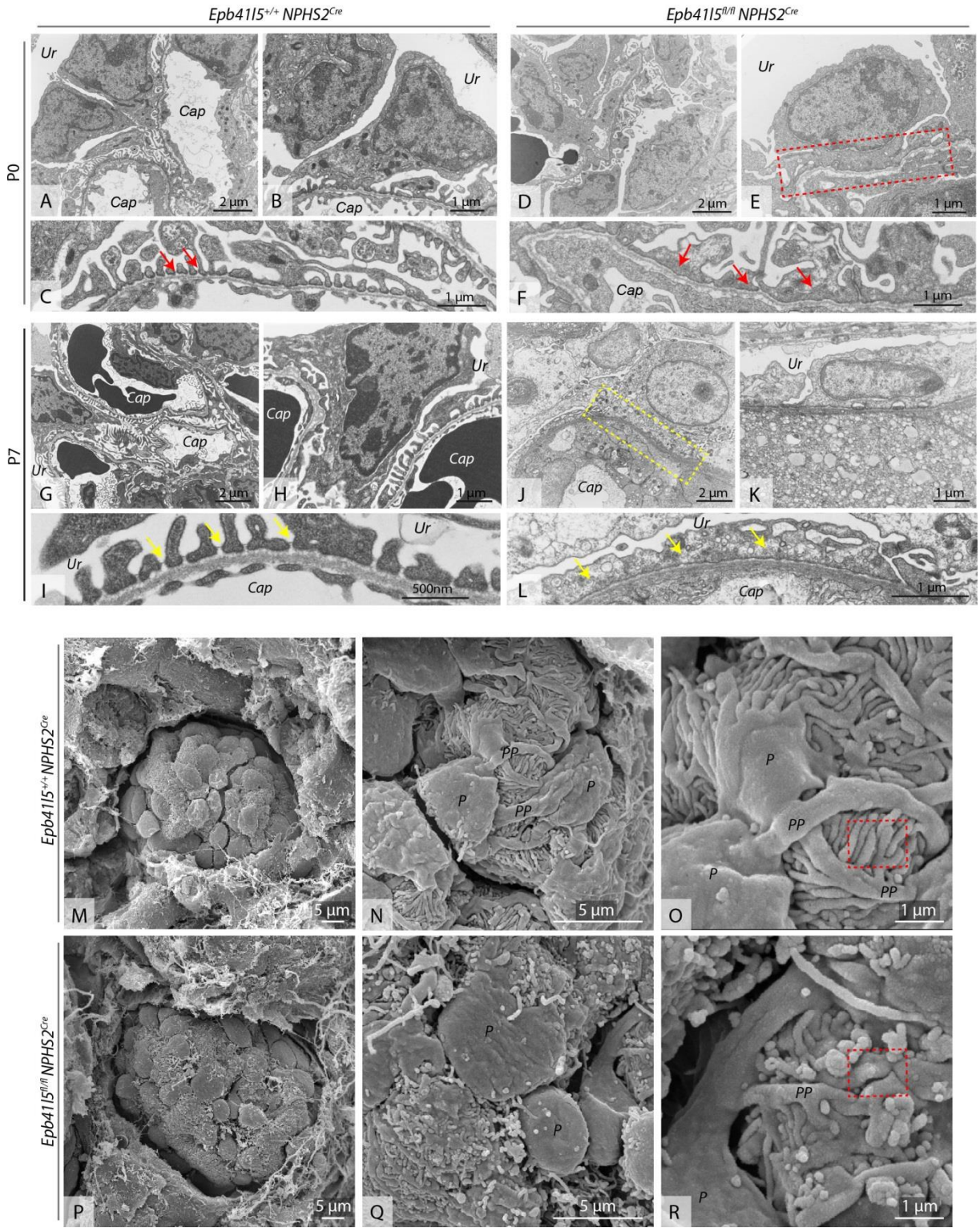

<u>Supplemental Figure 9</u>: *Epb41l5* knockout animals show severe signs of foot process effacement

(A-L) Electron microscopy revealed severe signs of global foot process fusion in *Epb41l5* knockout animals already at birth. One week after birth discrete vacuolization is noticed and slit diaphragms are not discernible any more (red arrows indicate fused areas of podocyte FPs; yellow arrows highlight slit diaphragms in wild type animals and electron dense accumulations in knockout animals; boxed regions

indicate zoomed details, Ur: urinary space; Cap: capillaries). **(M-R)** Scanning electron microscopy of glomeruli from wild type and *Epb41l5* knockout animals: while wild type animals showed a regular pattern of interdigitating foot processes, these structures were simplified and retracted in *Epb41l5* knockout animals (P = podocyte cell body, PP = primary processes; boxed regions indicate areas of disturbed FP architecture).

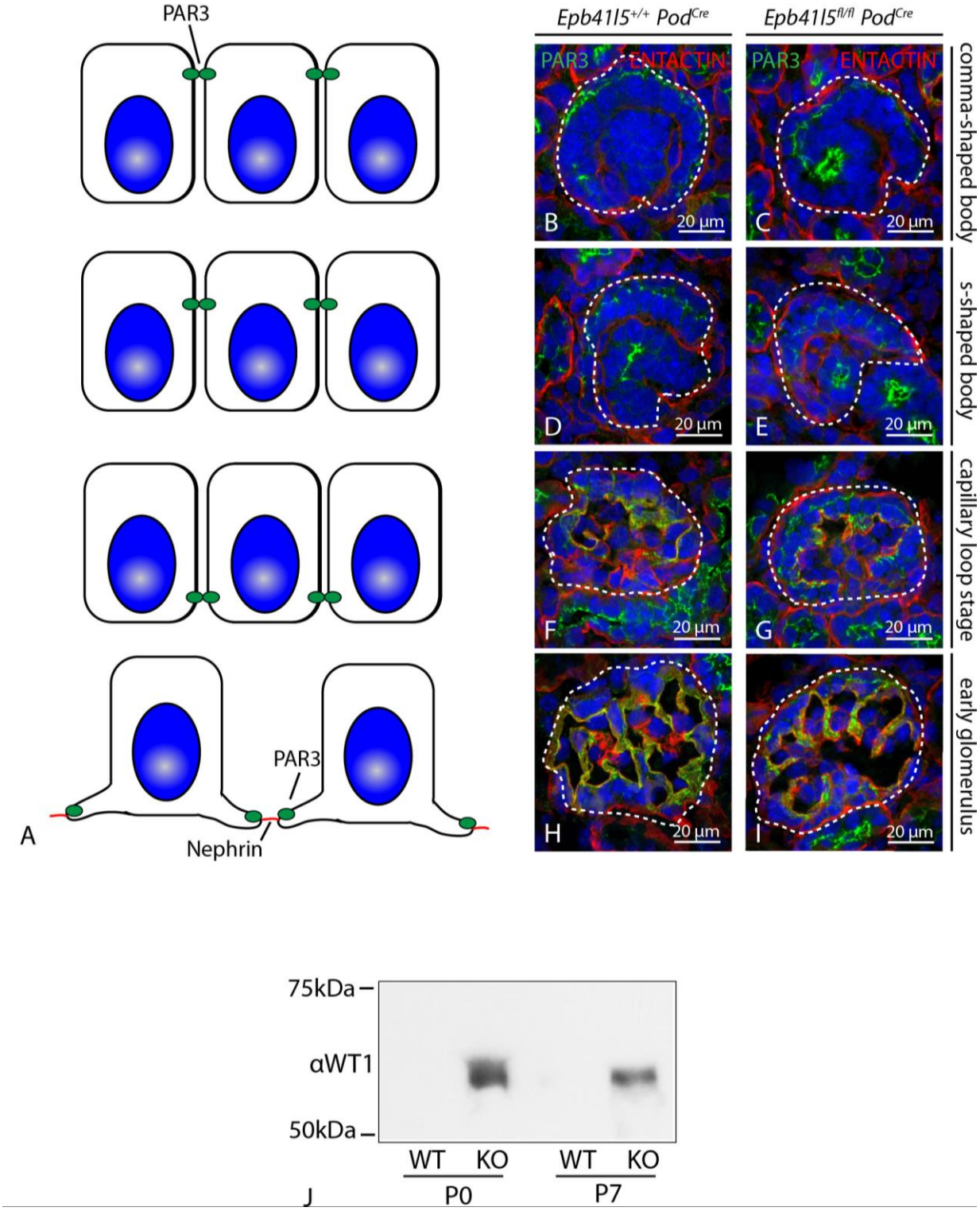

<u>Supplemental Figure 10</u>: Apico-basal migration of PAR3 is not influenced by EPB41L5 deficiency

(A) Schematic illustration of podocyte development: while transition from cuboidal epithelial cell morphology towards extensive basal specification and generation of podocyte foot processes certain marker proteins indicate the shift in polarization. PAR3 and slit diaphragm proteins like NEPHRIN migrate from the apical domain towards the basal compartment of podocytes. **(B-I)** The apico-basal migration of

PAR3 is not impaired in *Epb41l5* knockout mice. At the comma and s-shaped stage PAR3 is pre-dominantly apically localized (B-E). During further glomerular maturation PAR3 undergoes a change in localization towards the more basal compartment. No major alterations between wild type and respective knockout animals were observed at any developmental stage (*PodCre* was used synonymously used for *hNPHS2Cre*). **(J)** Western blot of urine samples detected a WT-1 positive band only in *Ebp41l5* knockout animals.

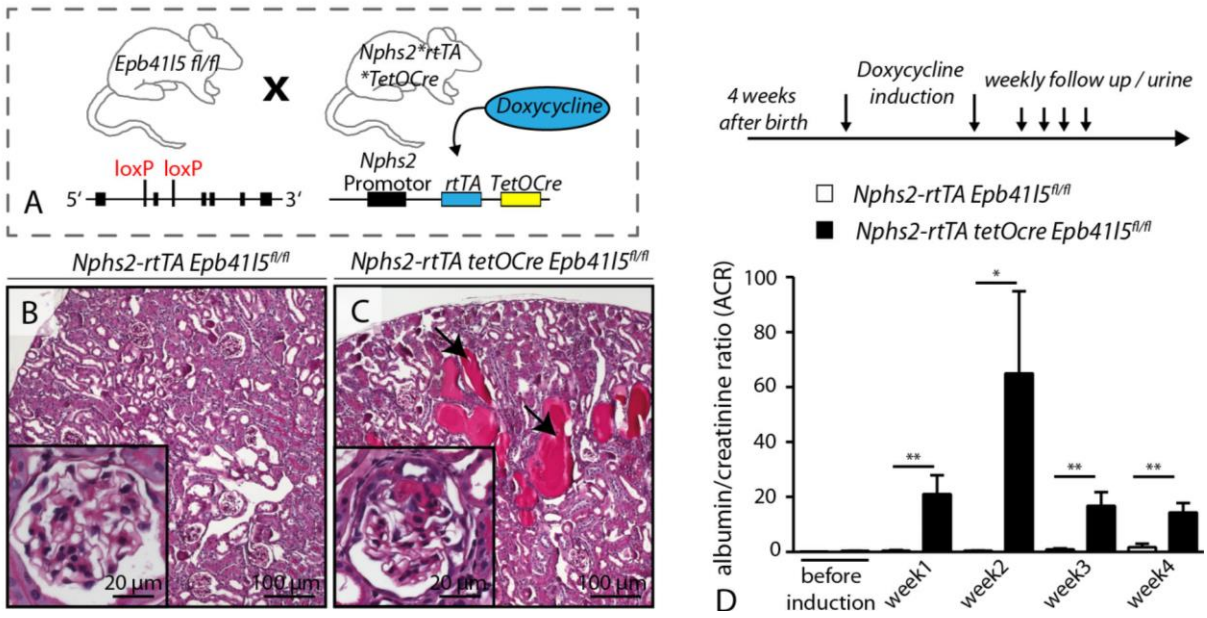

<u>Supplemental Figure 11</u>: Inducible deletion of *Epb41l5* in podocytes leads to nephrotic syndrome

(A) Schematic for the breeding strategy to generate inducible podocyte specific *Epb41l5* knockout mice (left panel). With the age of 4 weeks mice were induced with doxycycline via drinking water and after a 2 week induction protocol, weekly follow up monitored for levels of proteinuria (right panel). **(B-C)** Histology of induced *Epb41l5* knockout mice revealed accumulation of proteinaceous casts, dilated tubuli and segmental sclerosis in glomeruli (arrows and inserts). **(D)** Measurement of albumin/creatinine ratio revealed early onset of proteinuria already at 1 week after induction, further increasing at week 2 (after initial induction period at least 6 animals per genotype and time point were analyzed; for statistics see the material and methods section).

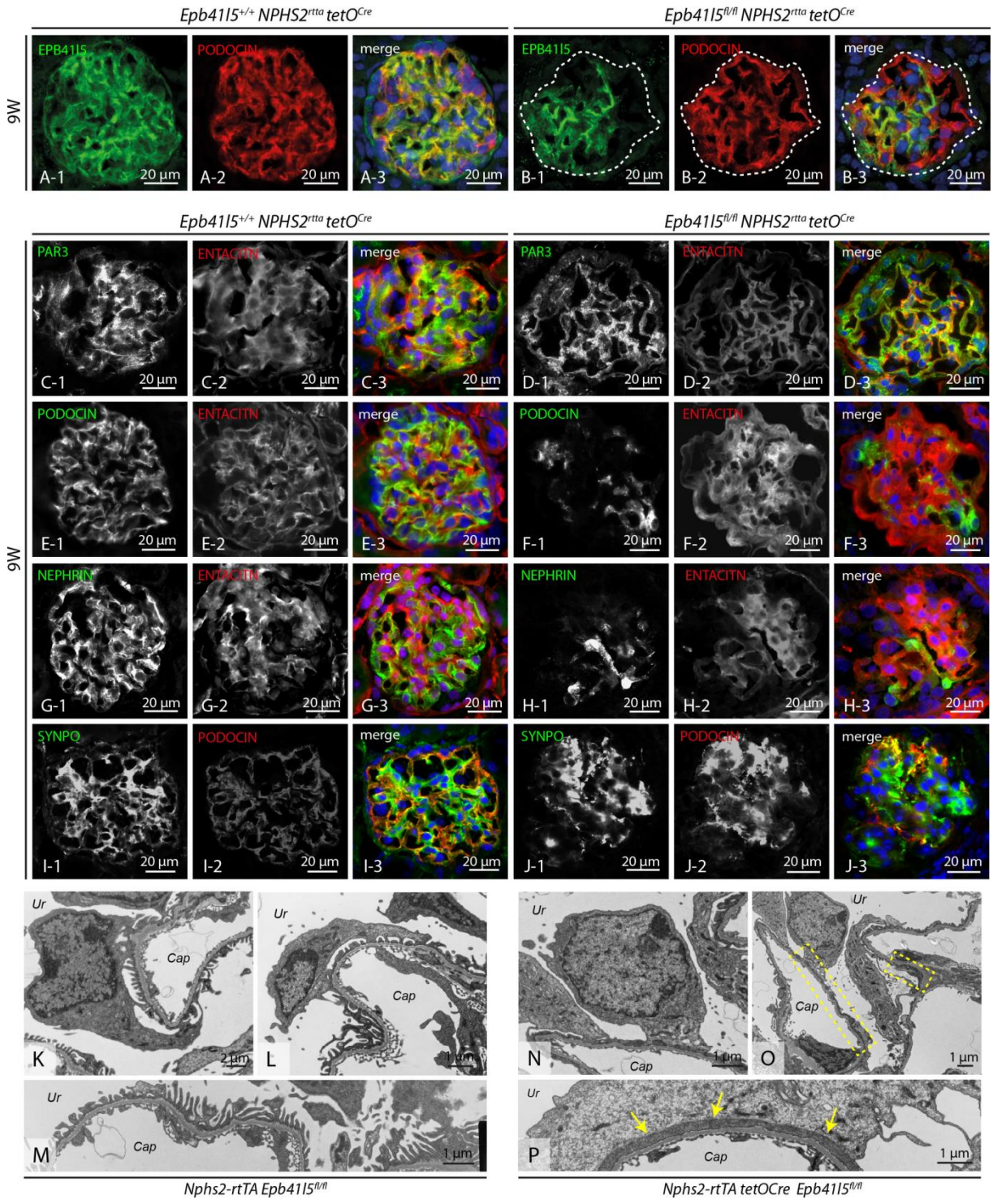

<u>Supplemental Figure 12</u>: Inducible deletion of *Epb41l5* in podocytes results in altered expression patterns of podocyte marker proteins.
(A&B) Immunofluorescence staining confirmed that EPB41L5 protein is reduced in *hNPHS2^{rtTA} tetO^{Cre} EPB41L5$^{fl/fl}$* animals. Due to incomplete recombination residual EPB41L5 protein was detectable in some podocytes. **(C-J)** After 5 weeks of induction typical slit diaphragm markers like PODOCIN and NEPHRIN showed a severely altered localization pattern, most likely due to heavy proteinuria in respective knockout animals **(E-H)**. In contrast, PAR3 showed only modest changes in localization and staining intensity **(C-D)**. In accordance with the massively disturbed

slit diaphragm proteins, also the cytoskeletal component SYNAPTOPODIN showed altered localization patterns **(I-J)**. **(K-P)** Electron microscopy revealed drastic alterations of FP morphology in respective induced knockout animals (boxed areas indicate zoomed details; yellow arrows highlight fused foot processes; Cap – capillaries; Ur – urinary space).

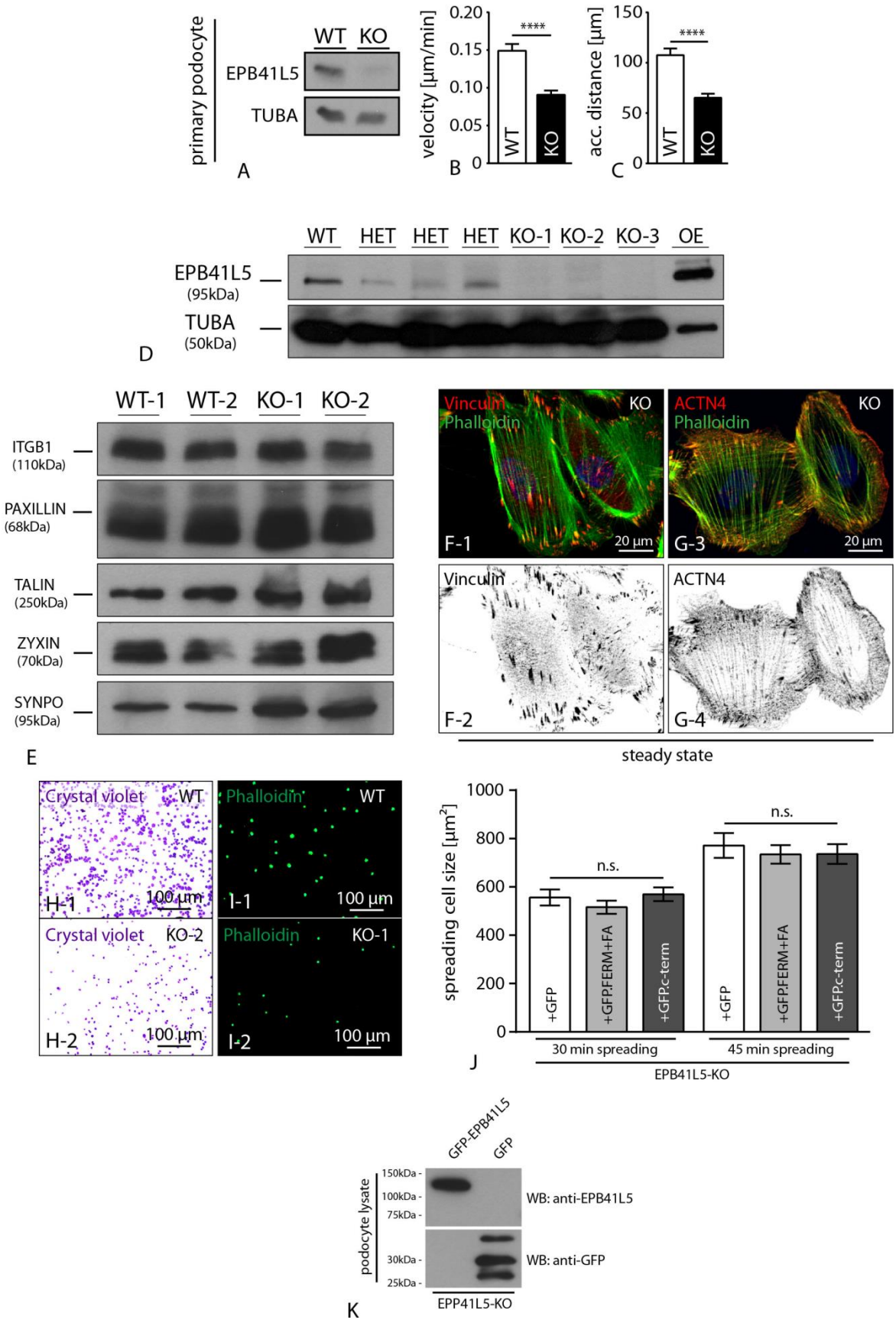

<u>Supplemental Figure 13</u>: Characterization of EPB41L5 knockout cell clones
(A-C) Western blot confirmed loss of EPB41L5 protein in primary podocytes from *Epb41l5* knockout animals. Epb41l5 knockout podocytes exhibited a decreased

migratory speed compared to wild type cells (at least n=50 cells over 3 independent experiments; dataset S3). **(D)** Western blot on different wild type, heterozygous and knockout CRISPR/CAS9 clones confirmed loss of protein in respective knockout podocytes (OE = overexpression of *EPB41L5*). **(E)** Western blot of wild type and *EPB41L5* knockout clones for different FA components did not detect major differences. **(F, G)** Staining for FA components VINCULIN and ACTININ-4 in *EPB41L5* knockout clones revealed normal morphology and no obvious alterations in terms of localization and intensity. **(H, I)** Overview images highlighting the different adhesion properties of respective EPB41L5 knockout clones compared to wild type controls. **(J)** Re-expression of FERM-domain as well as C-terminal EPB41L5 truncations were not capable of rescuing the spreading defect in EPB41L5 knockout cells (at least 87 cells were analyzed at both time points, for statistical data see dataset S3). **(K)** Western blot experiments confirm the efficient expression of GFP-tagged versions of EPB41L5 in transfected podocytes 48 post-transfection.

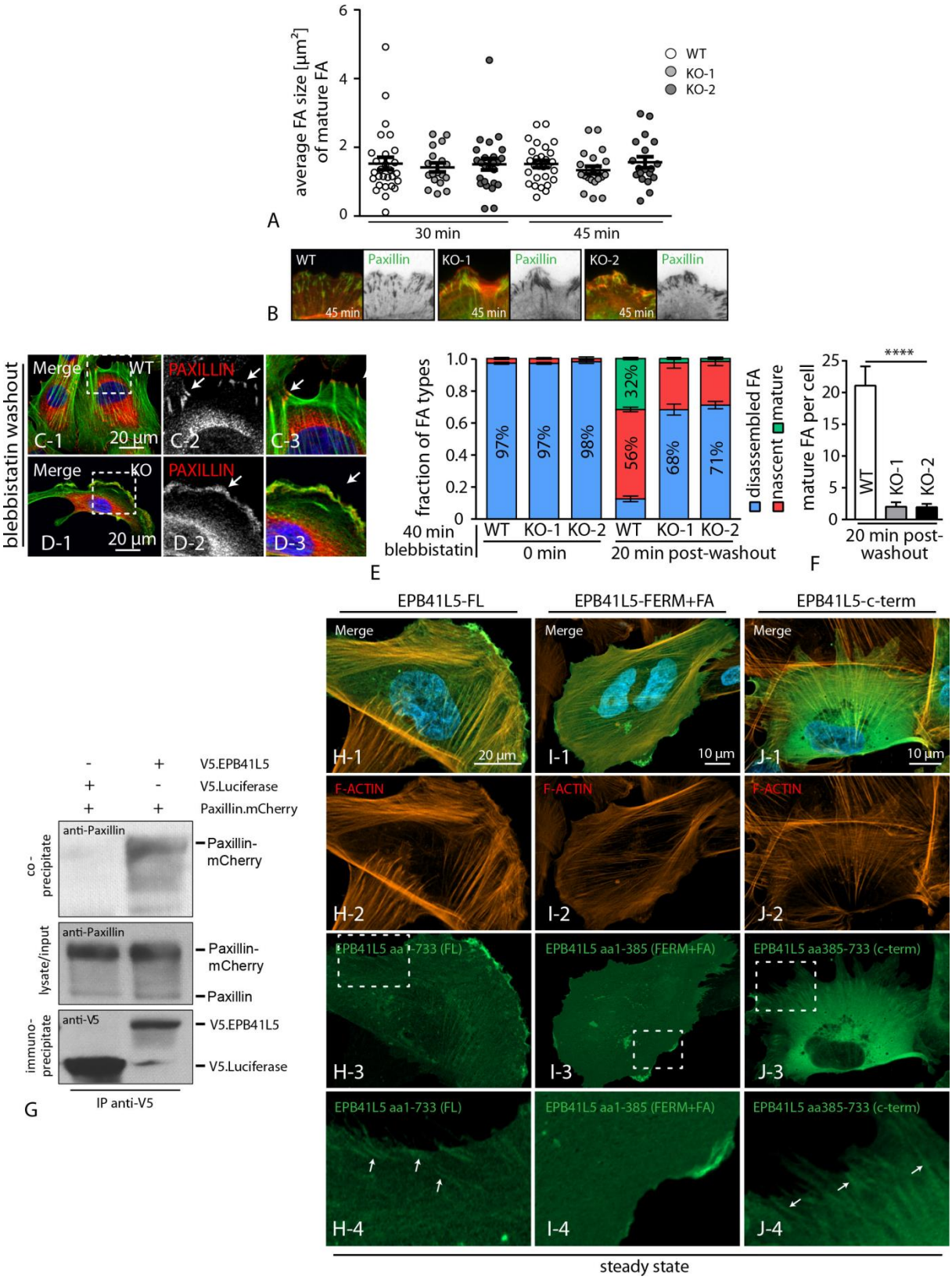

<u>Supplemental Figure 14</u>: EPB41L5 interacts with PAXILLIN

(A) Morphological analysis of focal adhesions at two different time points while cellular spreading detected no major differences between wild type and respective knockout clones (n=28, 18 and 25 at time point 30 minutes for WT, KO1 and KO2 respectively; n=28, 22 and 19 cells at time point 45 minutes for respective genotypes; averaged from 2 independent experiments, for statistical see dataset S3). **(B)**

PAXILLIN morphology at the leading edge of spreading cells at 45 minutes after spreading. **(C-E)** Impaired FA recovery after blebbistatin washout in knockout cells (more than 400 cells were analyzed; dataset S3). **(F)** Decreased number of mature FAs in *EPB41L5* KO cells after blebbistatin washout (n=20 cells, dataset S3). **(G)** Co-immunoprecipitation assay using epitope tagged versions of EPB41L5 and Paxillin in HEK293T cells, tagged luciferase was included as a control. **(H-J)** Expression of either full length, or FERM-domain as well as C-terminal truncations of EPB41L5 revealed that only the C-terminal part and the full-length version of EPB41L5 result in a FA localization pattern (white arrows). In contrast, the FERM-domain containing truncation showed a more membranous localization pattern (Phalloidin was used as a co-labeling; boxed areas indicate zoomed details).

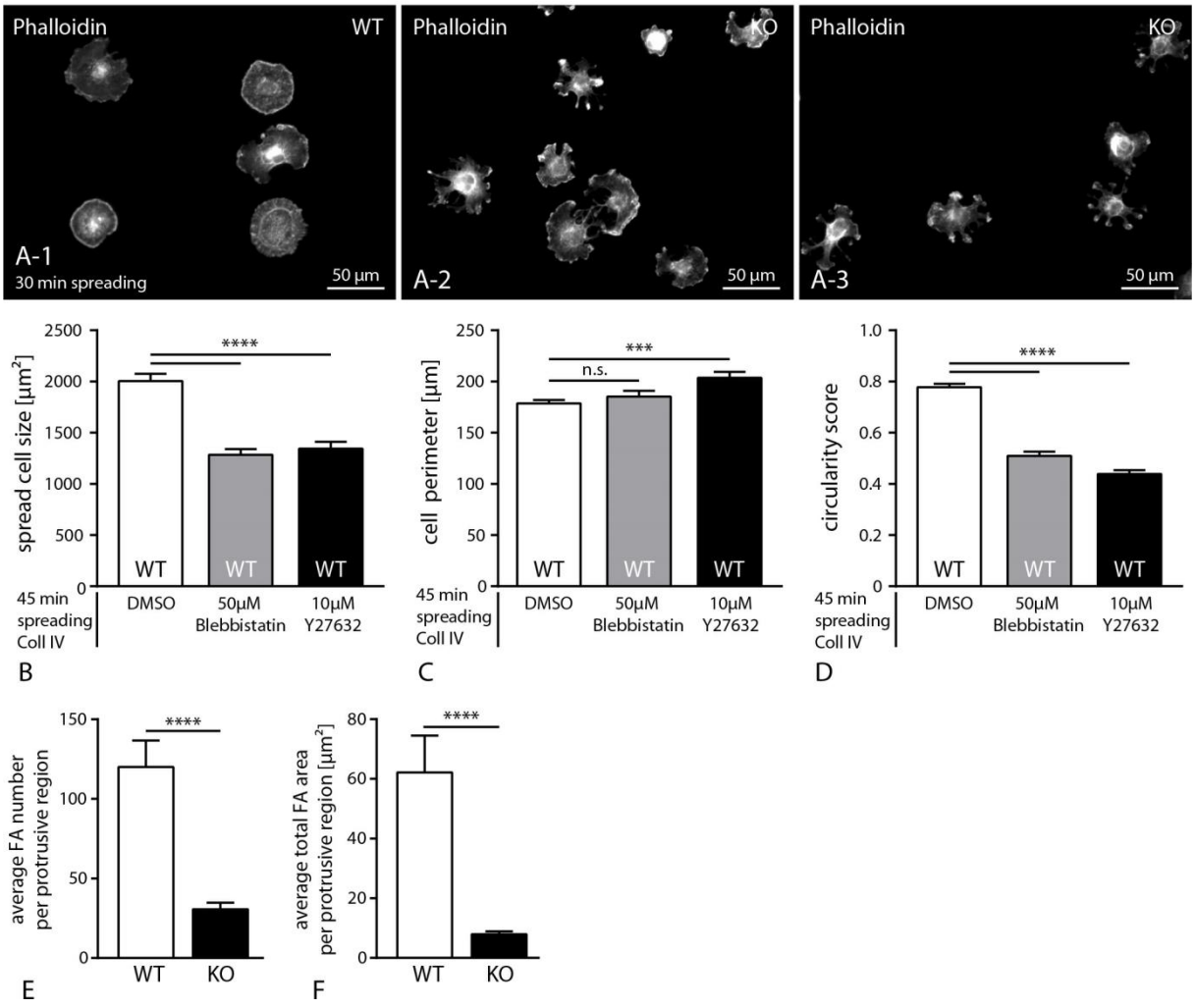

<u>Supplemental Figure 15</u>: Inhibition of the actomyosin machinery during dynamic cellular processes leads to a phenocopy of *Ebp41l5* knockout in wild type cells

(A) Representative images illustrating morphological difference between wild type and knockout cells while cellular spreading (30 min spreading on collagen IV coated glass cover slips; representative low magnification images from at least 5 independent experiments). **(B-D)** Quantification of cellular spreading size, perimeter and circularity of wild type cells pretreated with either blebbistatin or Y27632 during spreading (more than 150 cells per condition were quantified over 3 independent experiments; for statistics see the material and methods section). **(E, F)** Quantification of FA in pseudopods of spreading EPB41L5 knockout cells demonstrating lower FA numbers as well as decreased average total FA area (n=12 WT and 23 KO cells were analyzed, for statistics see dataset S3)

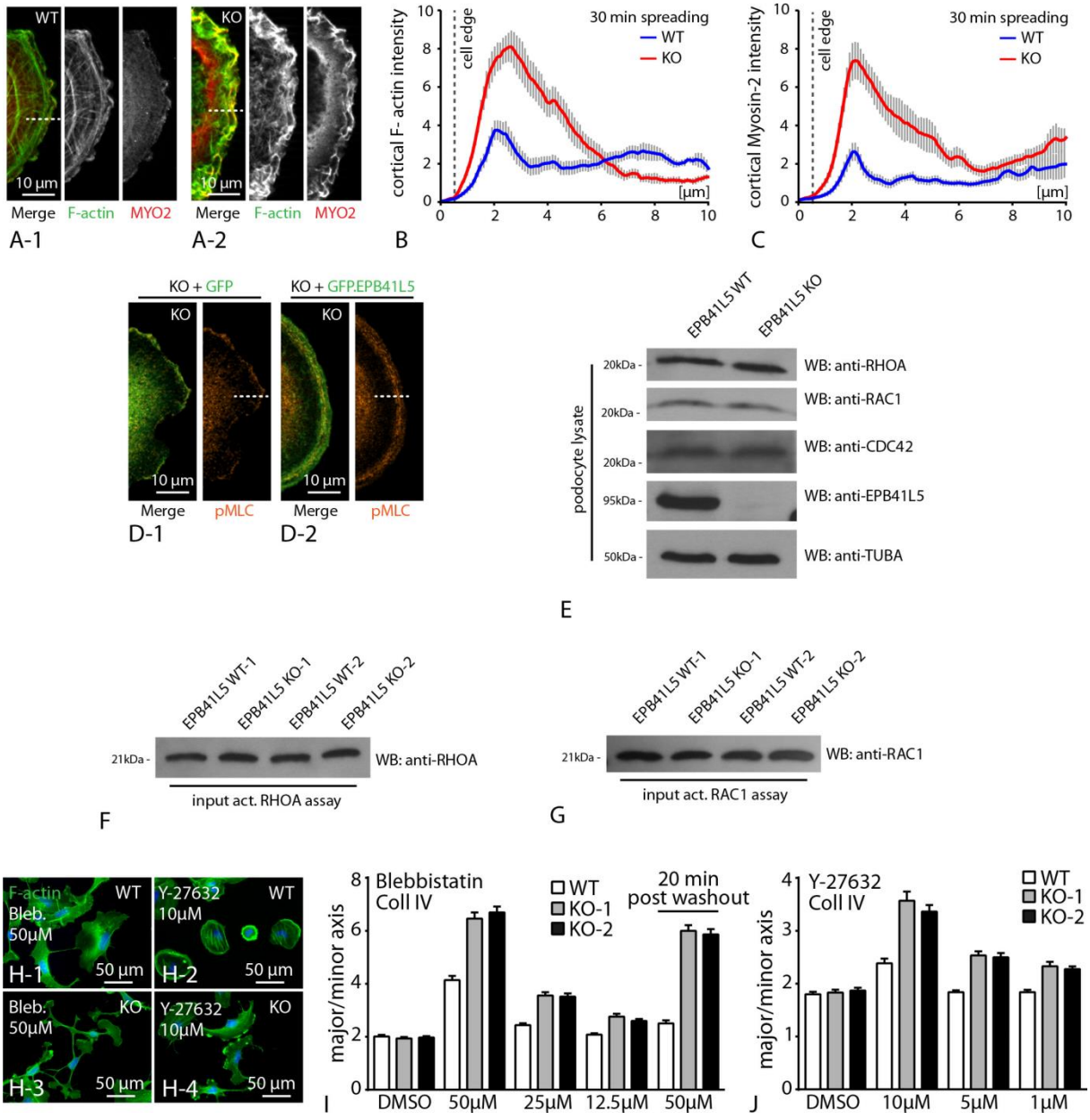

<u>Supplemental Figure 16</u>: Equal total levels of RhoA and RAC1 in EPB41L5 knockout cells

(A) Representative immunofluorescence for MYOSIN-II at the leading edge of wild type and EPB41L5 KO cells: accumulation of F-actin and MYOSIN-II was detected at the leading edge of KO cells. **(B-C)** Representative line scans for MYOSIN-II and F-actin across the cell edge (grey lines indicate respective SDs; at least 10 cells per condition). **(D)** Immunofluorescence for pMLC in EPB41L5 knockout cells with re-expression of full length EPB41L5 (white dotted line indicates area at the leading edge, selected for measurements represented in the main figures). **(E)** Western blot for various GTPases demonstrating equalized total levels between wild type and knockout cells. (**F, G)** Representative western blot for RhoA and Rac1 total levels out of equalized input lysates in G-Lisa assay. **(H-J)** Treatment with blebbistatin or Y-27632 led to pronounced morphological alterations in EPB41L5 KO cells when compared to wild type cells. (at least n=89 cells over 3 independent experiments; dataset S3).

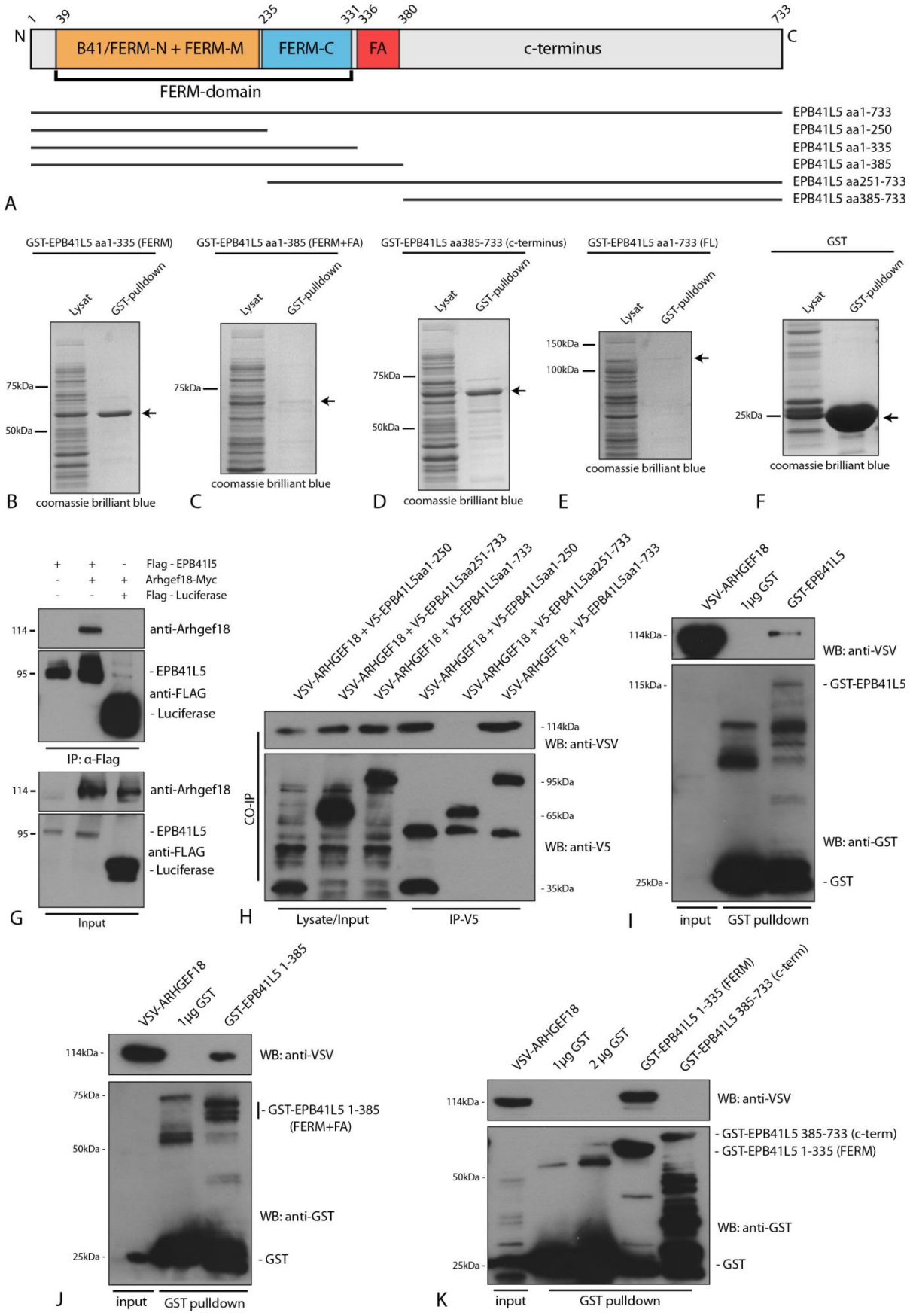
1
39
235
331
336
380
733
N
C
B41/FERM-N + FERM-M
FERM-C
FA
c-terminus
FERM-domain
EPB41L5 aa1-733
EPB41L5 aa1-250
EPB41L5 aa1-335
EPB41L5 aa1-385
EPB41L5 aa251-733
EPB41L5 aa385-733
A
GST-EPB41L5 aa1-335 (FERM)
GST-EPB41L5 aa1-385 (FERM+FA)
GST-EPB41L5 aa385-733 (c-terminus)
GST-EPB41L5 aa1-733 (FL)
GST
Lysat
GST-pulldown
75kDa
50kDa
150kDa
100kDa
25kDa
coomassie brilliant blue
B
C
D
E
F
+ + - Flag - EPB41l5
- + + Arhgef18-Myc
- - + Flag - Luciferase
114
95
anti-Arhgef18
- EPB41L5
anti-FLAG
- Luciferase
IP: α-Flag
Input
G
VSV-ARHGEF18 + V5-EPB41L5aa1-250
VSV-ARHGEF18 + V5-EPB41L5aa251-733
VSV-ARHGEF18 + V5-EPB41L5aa1-733
- 114kDa
WB: anti-VSV
- 95kDa
- 65kDa
WB: anti-V5
- 35kDa
CO-IP
Lysate/Input
IP-V5
H
VSV-ARHGEF18
1µg GST
GST-EPB41L5
114kDa -
115kDa -
25kDa -
WB: anti-VSV
- GST-EPB41L5
WB: anti-GST
- GST
input
GST pulldown
I
VSV-ARHGEF18
1µg GST
GST-EPB41L5 1-385
114kDa -
75kDa -
50kDa -
25kDa -
WB: anti-VSV
- GST-EPB41L5 1-385
(FERM+FA)
WB: anti-GST
- GST
input
GST pulldown
J
VSV-ARHGEF18
1µg GST
2 µg GST
GST-EPB41L5 1-335 (FERM)
GST-EPB41L5 385-733 (c-term)
114kDa -
50kDa -
25kDa -
WB: anti-VSV
- GST-EPB41L5 385-733 (c-term)
- GST-EPB41L5 1-335 (FERM)
WB: anti-GST
- GST
input
GST pulldown
K

<u>Supplemental Figure 17</u>: ARHGEF18 and EPB41L5 interaction studies
(A) Schematic depicting the domain structure of EPB41L5 and including the various used truncations. **(B-F)** Coomassie blue staining of respective GST-tagged truncated protein versions indicated different efficiencies in protein expression due to protein size (note FERM-domain and C-terminal truncations showed the best expression efficiency). **(G)** Co-immunoprecipitation assay with epitope tagged versions of EPB41L5 and ARHGEF18 in HEK293T cells, FLAG-tagged Luciferase was included as a control. Precipitated ARHGEF18 was detected using antibody directed against ARHGEF18. **(H)** Mapping studies using additional truncations of EPB41L5 together with overexpressed ARHGEF18; only full length EPB41L5 and the FERM-domain (FERM A+B/B41 domain) containing truncation was able to precipitate ARHGEF18. **(I-K)** GST-pulldown experiments using either full-length EPB41L5 recombinant protein, or respective truncations (FERM, FERM+FA, or C-terminal domain) in combination with epitope tagged ARHGEF18. Note: only the FERM-domain containing truncated protein versions showed successful pulldown of ARHGEF18.

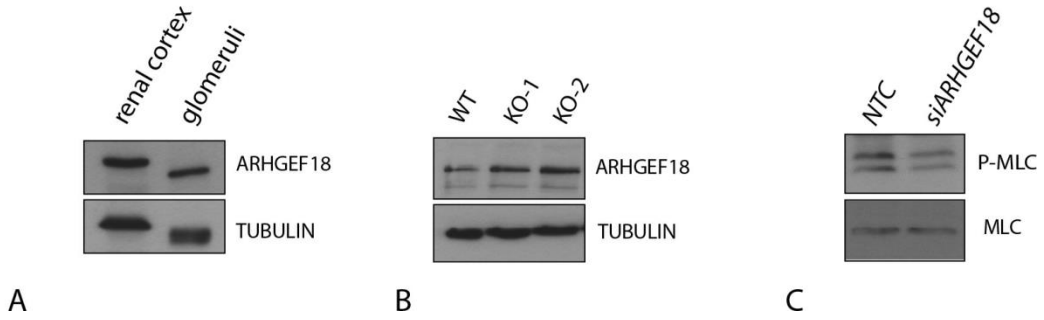

<u>Supplemental Figure 18</u>: ARHGEF18 expression in wild type murine kidneys and EPB41L5 knockout cells

(A) Western blot for ARHGEF18 in adult murine renal cortices and isolated glomeruli; TUBULIN was used as a loading control. **(B)** Western blot experiments for ARHGEF18 in EPB41L5 and wild type control cells revealed equal levels for ARGEFH18. **(C)** Decreased levels of p-MLC upon knockdown with ARHGEF18 siRNA; MLC total levels were used as input controls.

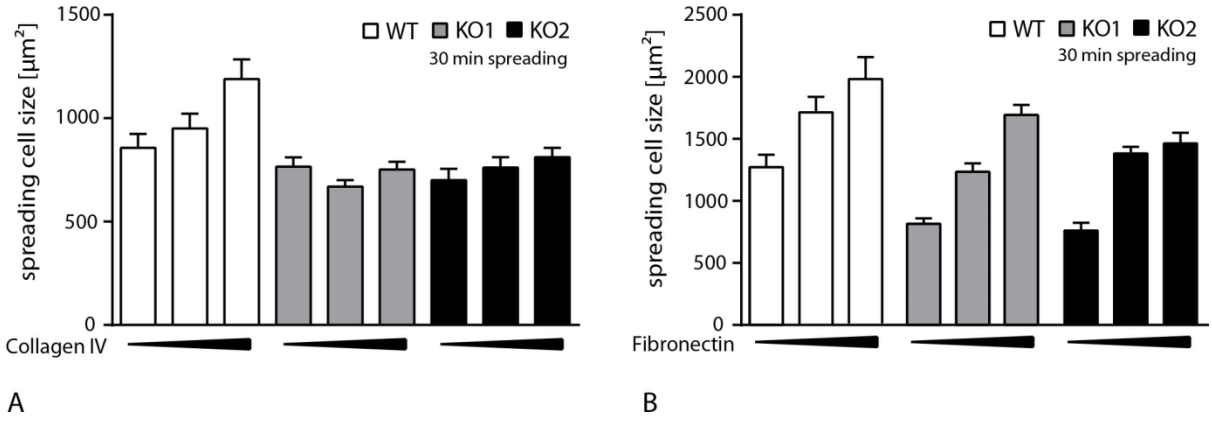

<u>Supplemental Figure 19</u>: ECM composition and concentration differentially influences EPB41L5 dependent spreading defect

(A, B) Analysis of cell spreading depending on ECM coating and concentration (collagen IV and fibronectin): A clear response to increasing fibronectin concentrations was observed in wild type cells as well as knockout clones. This response was partially observed also on collagen IV, but here solely in wild type cells (one representative experiment out of 3 independent experiments, for statistics see dataset S3).

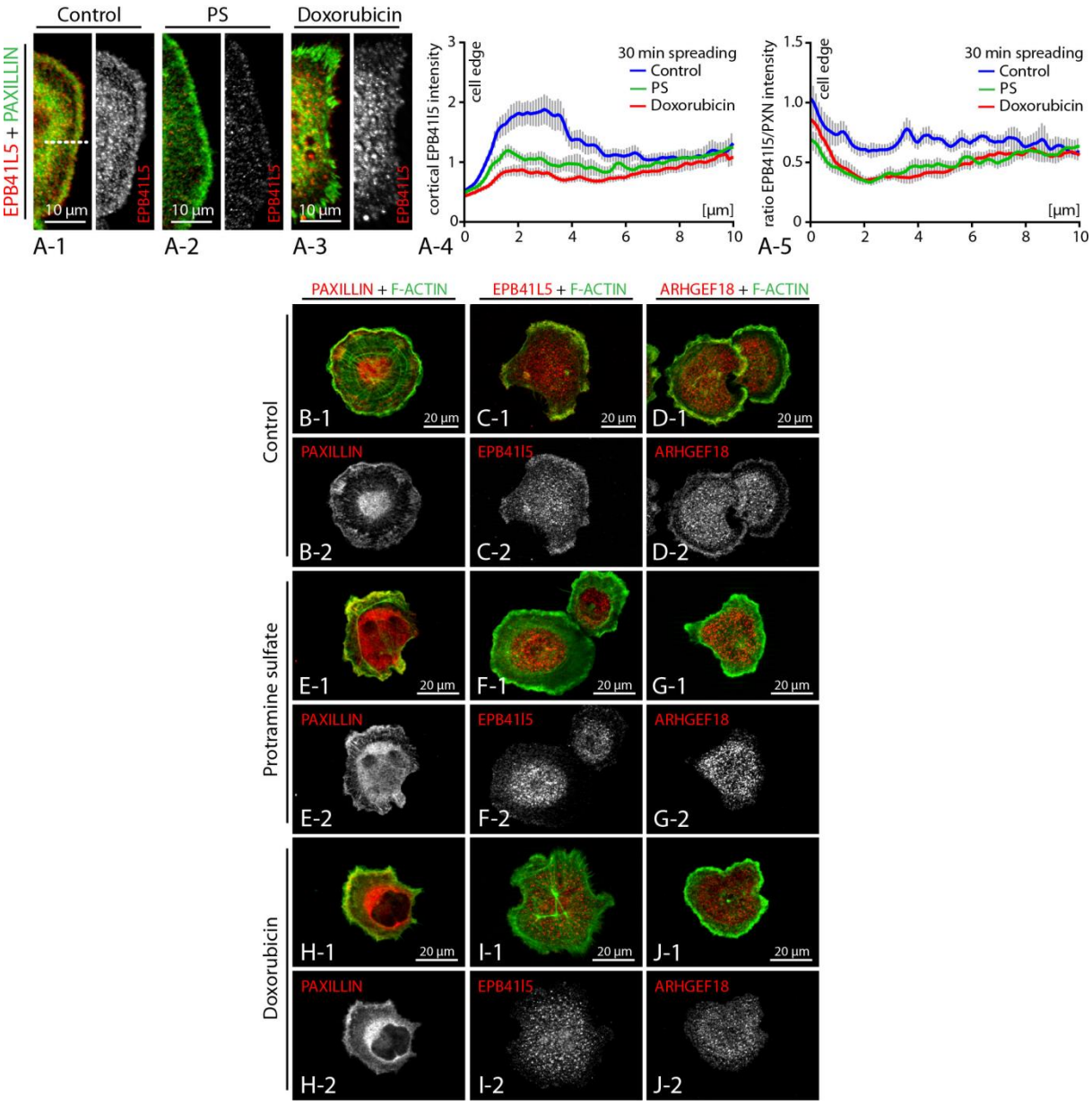

<u>Supplemental Figure 20</u>: EPB41L5 is sensitive towards podocyte toxic substances

(A) Immortalized human podocytes were treated with either protamine sulfate or doxorubicin and stained for EPB41L5 and PAXILLIN. Compared to control cells EPB41L5 exhibited a decreased signal intensity at the leading edge of either PS or doxorubicin treated cells as highlighted in depicted line scans (A4 and A5). **(B-J)** EPB41L5 as well as ARHGEF18 localize towards the leading edge in spreading podocytes. Treatment with podocyte toxic substances such as protamine sulfate or doxorubicin resulted in diminished signal intensity for both proteins, whereas F-actin was still present at the leading edge zone.

Supplemental Movies S1-S5

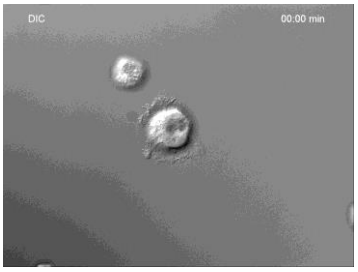

Movie S1 – EPB41L5 KO – DIC

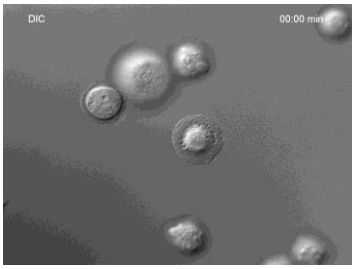

Movie S2 – Wild type podocyte – DIC

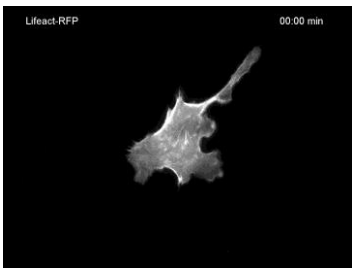

Movie S3 – EPB41L5 KO – Lifeact-RFP

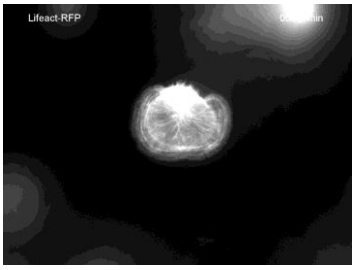

Movie S4 – Wild type podocyte – Lifeact-RFP

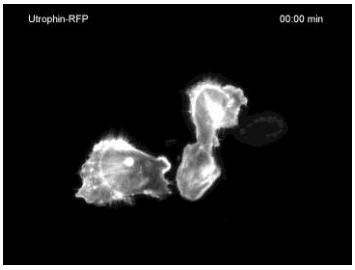

Movie S5 – EPB41L5 KO – Utrophin-RFP

<u>Supplemental Movies S1-5</u>: Visualization of spreading EPB41L5 KO and wild type cells, using DIC, Life-Act-RFP and Utrophin-RFP

Live cell imaging of spreading EPB41L5-KO and WT cells was performed using differential interference contrast (*DIC*) microscopy or fluorescence microscopy employing either Life-Act-RFP or Utrophin-RFP as actin probes.

Supporting Information -
Antibodies

Protein	Clone	Species	Manufacturer	Application
act. INTEGRIN-beta1	9EG7	rat	BD Transduction Lab.	WB (1:1000)
ACTININ-4		rabbit	Abcam	IF (1:200), WB (1:1000)
ARHGEF18		rabbit	Origene	IF (1:100)
ARHGEF18	HPA042689	rabbit	Atlas Antibodies	IF (1:100), WB (1:1000), IP (1:100)
B-ACTIN		mouse	Sigma	WB (1:1000)
CDC42	sc-87	rabbit	Santa Cruz	WB (1:1000)
CRUMBS3		rabbit	Sigma	IF (1:100)
EPB41L5	HPA037563	rabbit	Atlas Antibodies	IF (1:100), WB (1:500)
EPB41L5	HPA037564	rabbit	Atlas Antibodies	IF (1:50)
EPB41L5		rb,gp	gen. gift R. Roepman	IF (1:100), WB (1:1000)
FLAG	M2	mouse	Sigma	WB (1:1000)
FLNA	sc-28284	rabbit	Santa Cruz	WB (1:1000)
GFP	sc-9996	mouse	Santa Cruz	WB (1:1000)
GST	27-4577-01	goat	amersham pharmacia biotech	WB (1:1000)
INTEGRIN-beta1	M-106	rabbit	Santa Cruz	WB (1:1000)
ITGA2	AB1936	rabbit	Millipore	WB (1:1000)
ITGAV	ab179475	rabbit	Abcam	WB (1:1000)
MLC	3672	rabbit	Cell Signaling	WB (1:1000)
MYOSIN-II		rabbit	Covance	IF (1:100)
MYPT1	8574	rabbit	Cell Signaling	WB (1:1000)
NEPHRIN	gp-N2	gp	Progene	IF (1:300)
NIDOGEN	MAB1946	rat	Millipore	IF (1:300)
PAR3		rabbit	Millipore	IF (1:100)
PAXILLIN		mouse	BD Transduction Lab.	IF (1:300),WB (1:1000)
P-MLC	3674	rabbit	Cell Signaling	IF (1:100), WB (1:500)
P-MLC	3671	rabbit	Cell Signaling	IF (1:100), WB (1:500)
pMYPT1	5163	rabbit	Cell Signaling	WB (1:500)
PODOCALYXIN		mouse	gift from Tsilibary E	IF (1:100)
PODOCIN		rabbit	Sigma	IF (1:200)
P-PAXILLIN	2541	rabbit	Cell Signaling	WB (1:1000)
RAC1	240106	mouse	Cell Biolabs	IF (1.100) WB (1:1000)
RHOA	ARH03	mouse	Cytoskeleton	IF (1:100), WB (1:500)
SCRIBBLE		rabbit	Santa Cruz	IF (1:125)
SYNAPTOPODIN		mouse	Progene	IF (1:300)
TALIN		mouse	Sigma	IF (1:100)
TUBULIN		mouse	Sigma	WB (1:1000)
V5	MCA1360	mouse	Serotec	WB (1:1000), IP(1:2000)
VINCULIN	SPM227	mouse	Abcam	IF (1:100), WB (1:1000)
VSV	ab18612	rabbit	Abcam	WB (1:1000), IP(1:1000)
WT-1	clone 6F-H2	mouse	Millipore	IF (1:200), WB (1:1000)
ZYXIN	HPA004835	rabbit	Atlas Antibodies	IF (1:100)

Anti-Flag M2 Agarose Affinity beads			Sigma	IP (25µl/1ml Lysate)
Glutathione Sepharose			GE Healthcare	IP (25µl/1ml Lysate)

Supporting Information – uncropped Western Blots

F3D
WB: EPB41l5

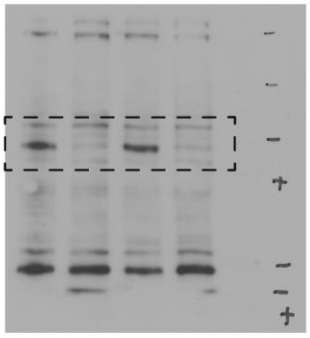

F3D
WB: TUBA

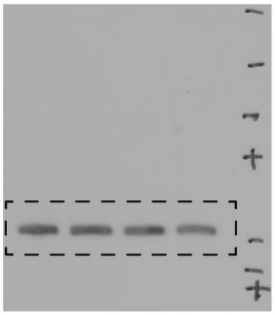

F3P
WB: WT1

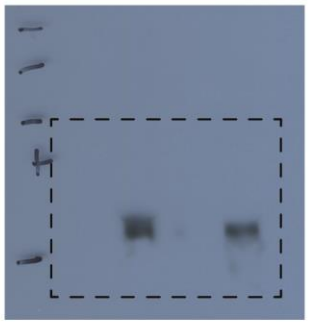

F3R
WB: EPB41L5

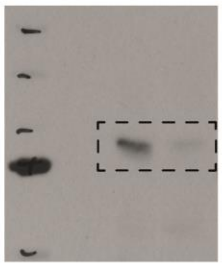

F3R
WB: TUBA

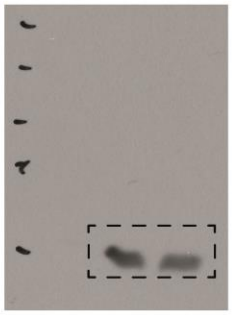

F4B
WB: EPB41L5

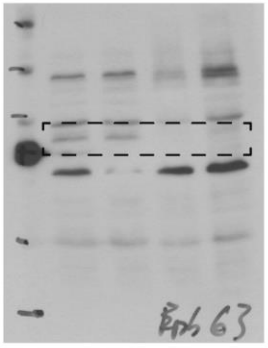

F4B
WB: TUBA

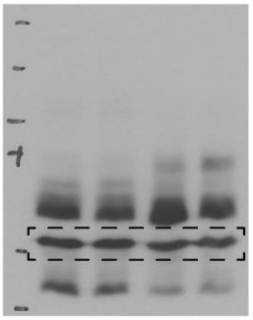

F4Q
WB: GST

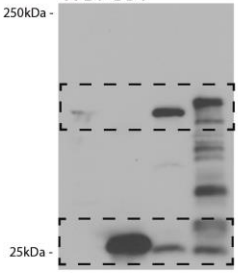

F4Q
WB: PAXILLIN

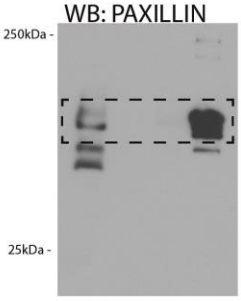

F4Q
WB: ITGB1

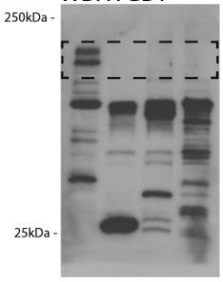

F4Q
WB: ITGAV

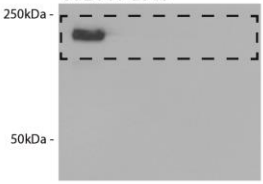

F5R
WB: p-MLC

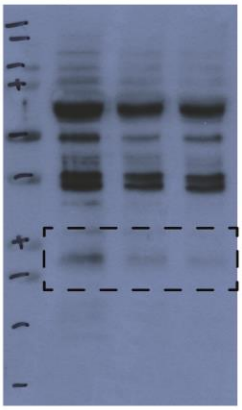

F5R
WB: MLC

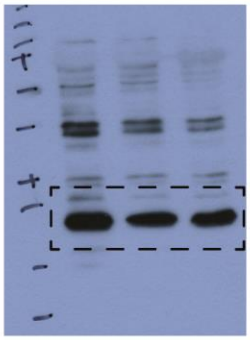

F5R
WB: TUBA

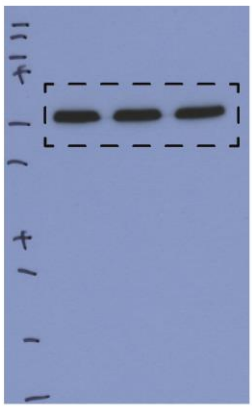

F5R
WB: p-MYPT1

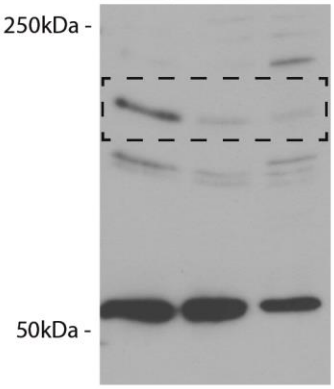

F5R
WB: MYPT1

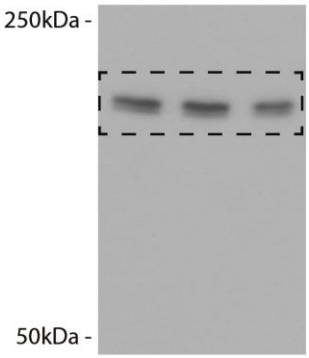

F5W
WB: p-MLC

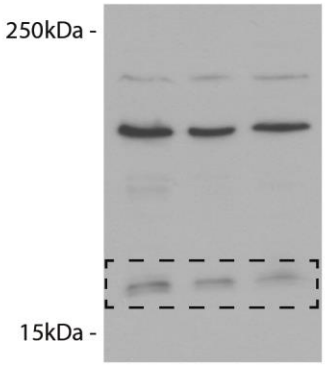

F5W
WB: MLC

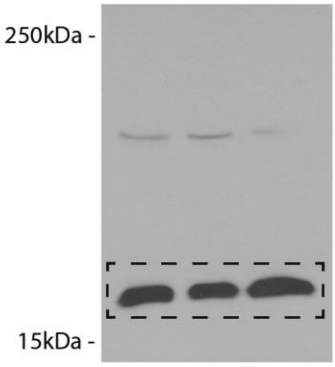

F5W
WB: p-MYPT1

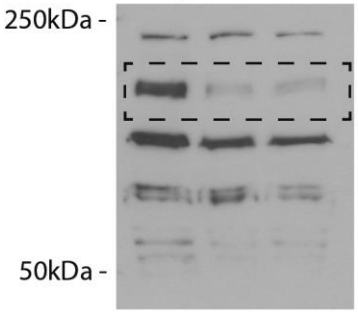

F5W
WB: MYPT1

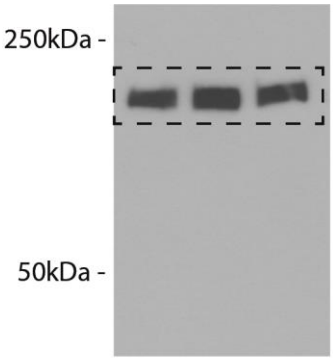

F5W
WB: TUBA

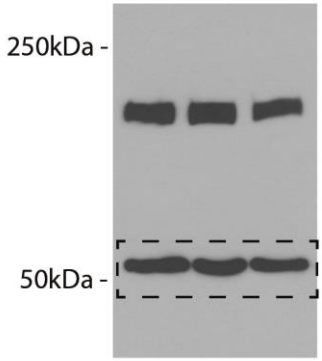

F6B
WB: EPB41L5

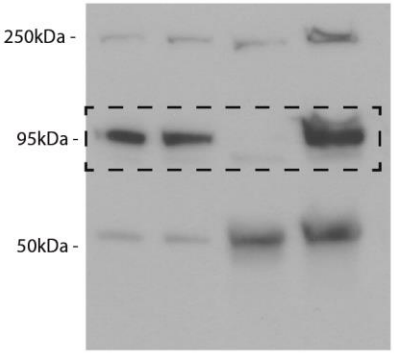

F6B
WB: ARHGEF18

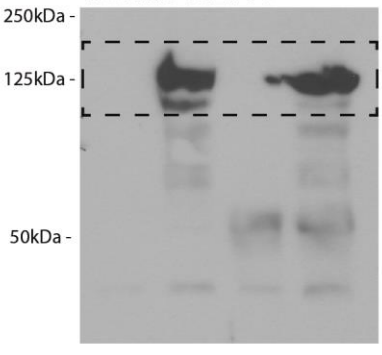

F6B
WB: GFP

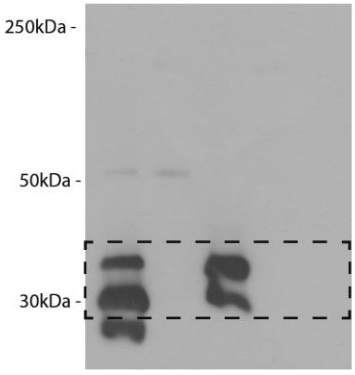

F6C
WB: ARHGEF18

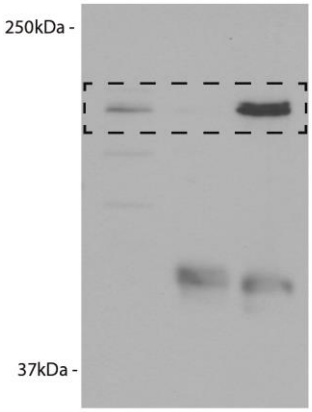

F6C
WB: EPB41L5

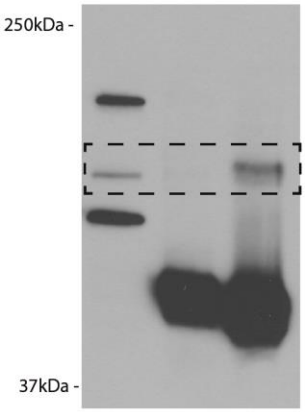

F6D
WB: VSV

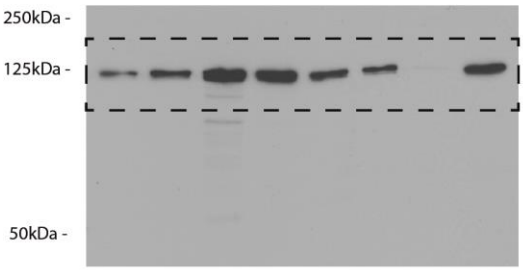

F6D
WB: FLAG

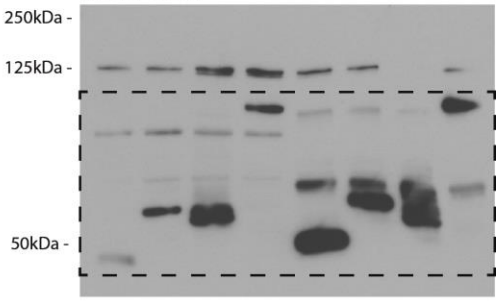

F6E
WB: ARHGEF18

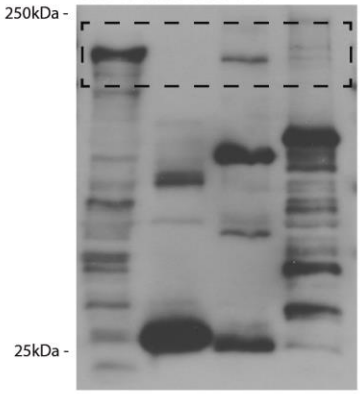

F6E
WB: GST

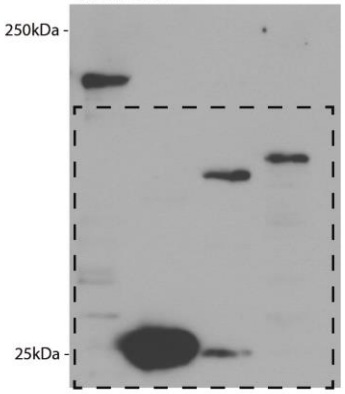

F6F
WB: ARHGEF18

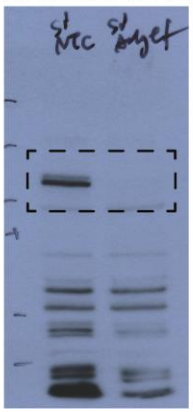

F6F
WB: TUBA

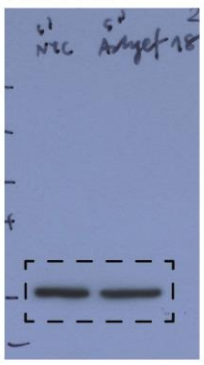

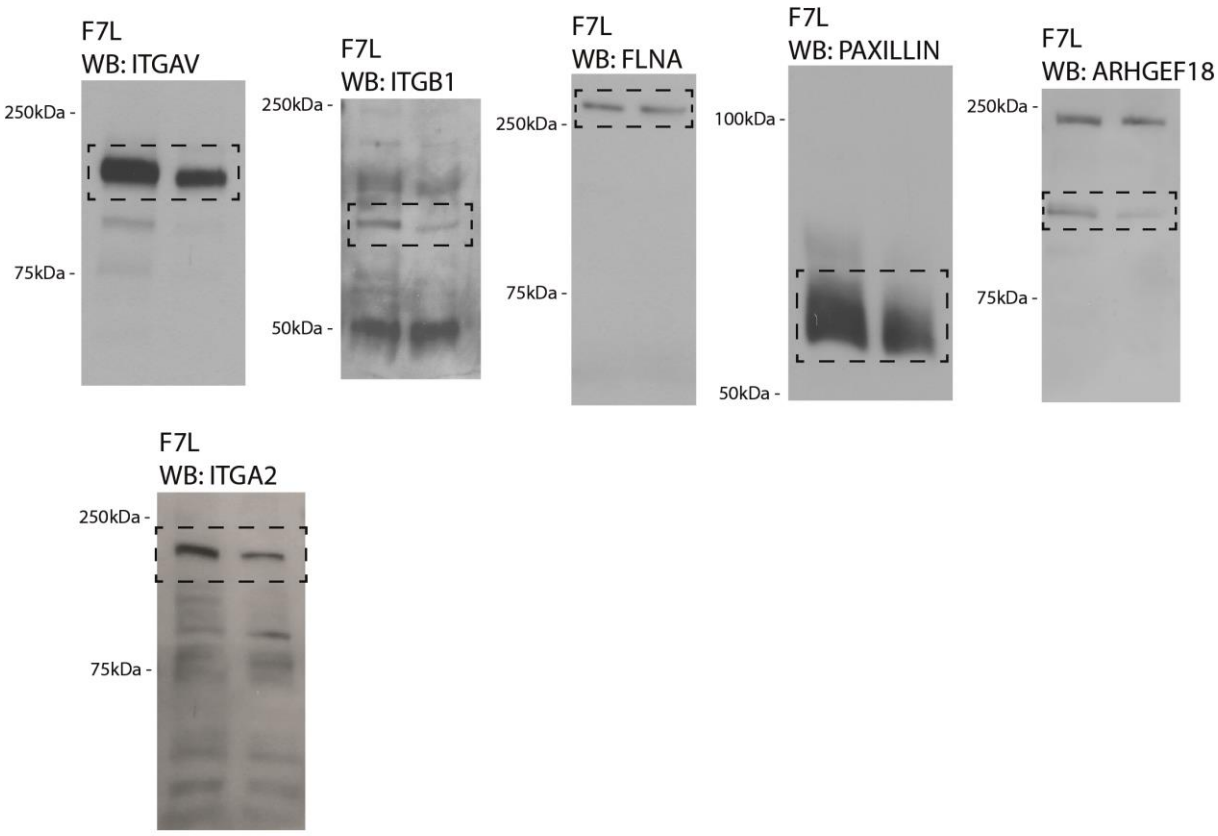
F7L
WB: ITGAV
250kDa -
75kDa -
F7L
WB: ITGB1
250kDa -
50kDa -
F7L
WB: FLNA
250kDa -
75kDa -
F7L
WB: PAXILLIN
100kDa -
50kDa -
F7L
WB: ARHGEF18
250kDa -
75kDa -
F7L
WB: ITGA2
250kDa -
75kDa -

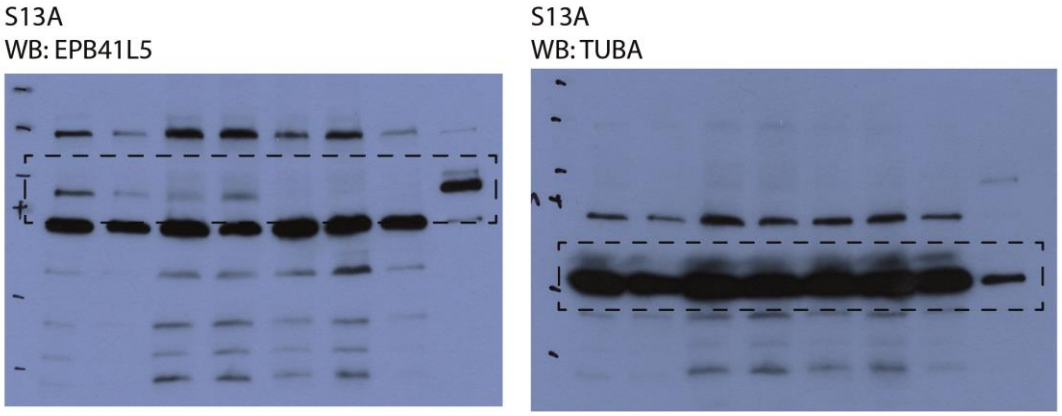
S13A
WB: EPB41L5
S13A
WB: TUBA

S13B
WB: SYNPO

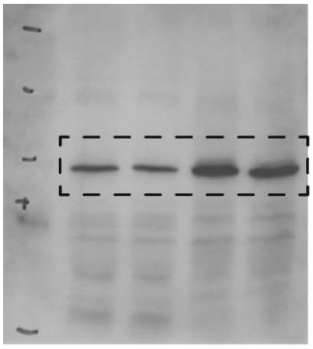

S13B
WB: Talin

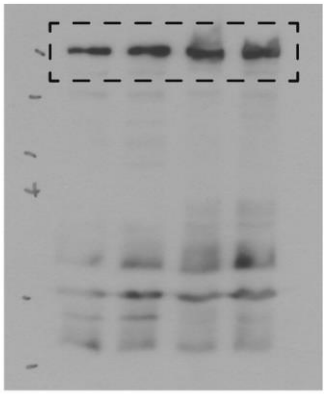

S13B
WB: Paxillin

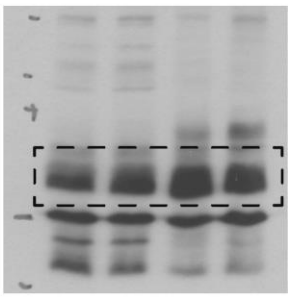

S13B
WB: ITGB1

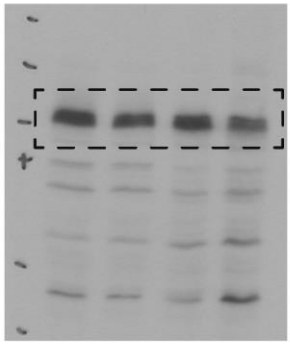

S13B
WB: Zyxin

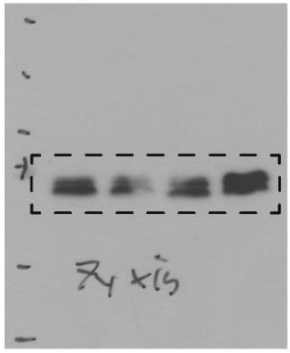

S13G
WB: EPB41L5

S13G
WB: GFP

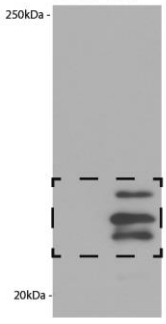

S14A
WB: Paxillin

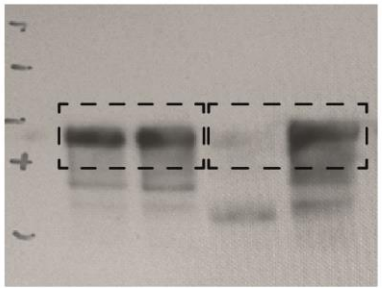

S14A
WB: V5

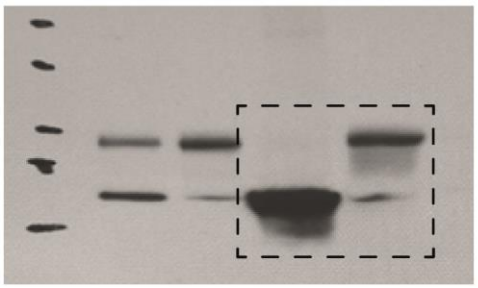

S16E
WB: RAC1

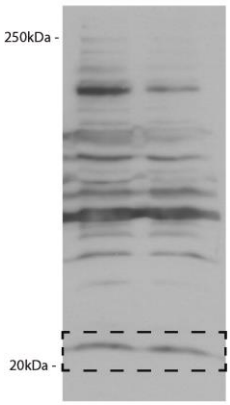

S16E
WB: CDC42

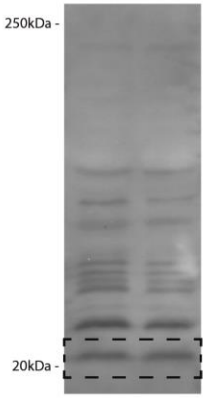

S16E
WB: RHOA

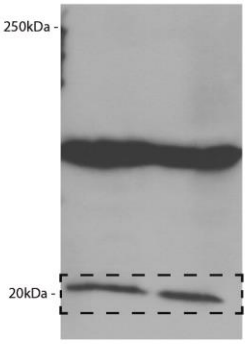

S16E
WB: TUBA

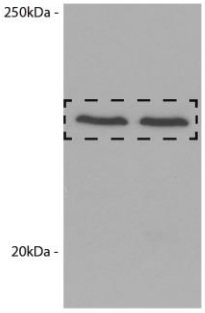

S16E
WB: EPB41L5

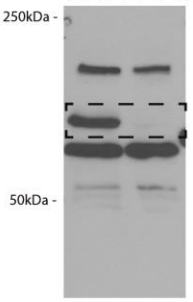

S16F
WB: RHOA

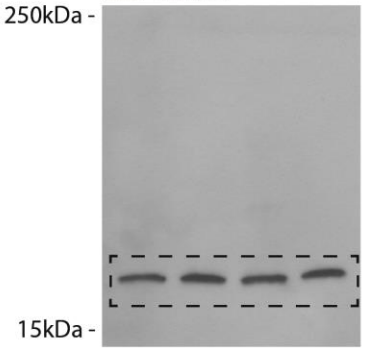

S16G
WB: RAC1

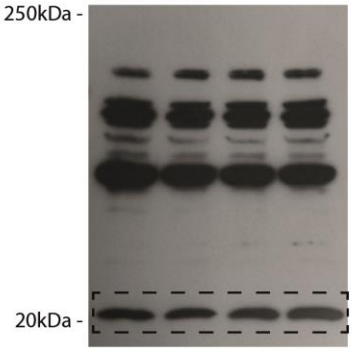

S17G
WB: ARHGEF18

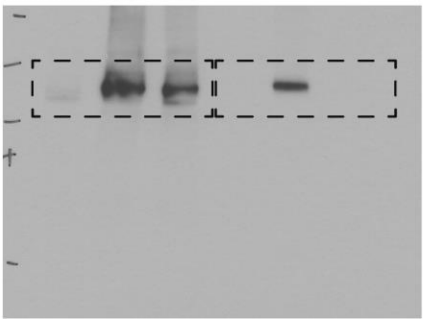

S17G
WB: FLAG

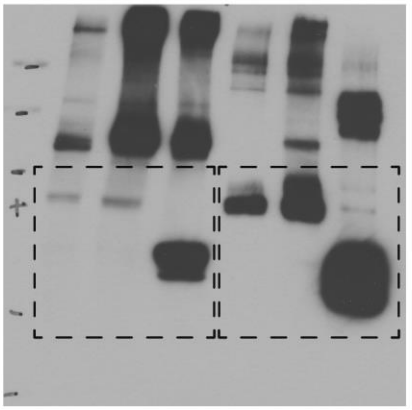

S17H
WB: V5

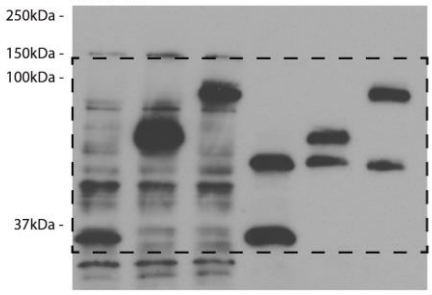

S17H
WB: VSV

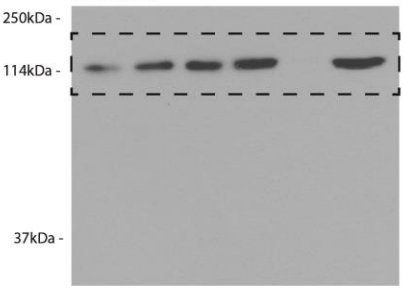

S17I
WB: VSV

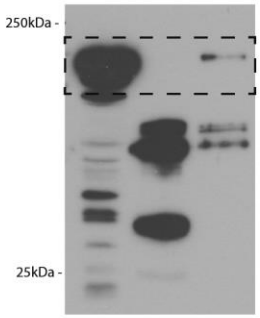

S17I
WB: GST

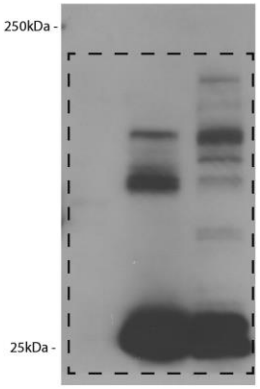

S17J
WB: GST

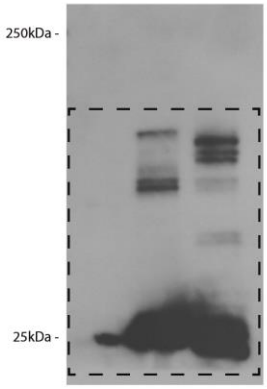

S17J
WB: VSV

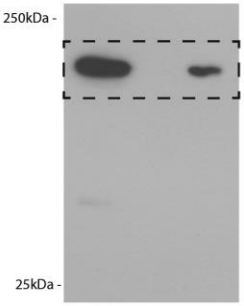

S17K
WB: VSV

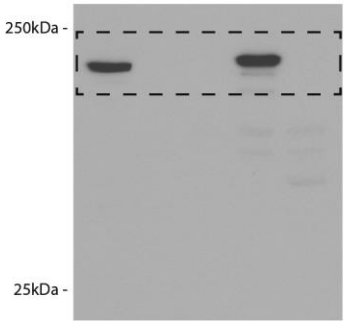

S17K
WB: GST

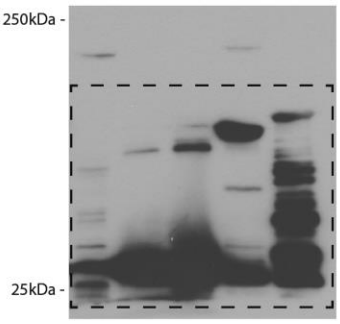

S18A
WB: ARHGEF18

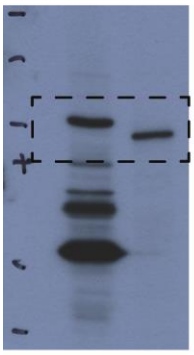

S18A
WB: TUBA

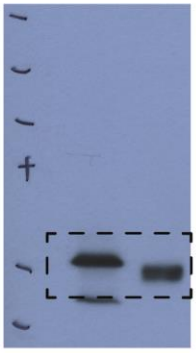

S18B
WB: ARHGEF18

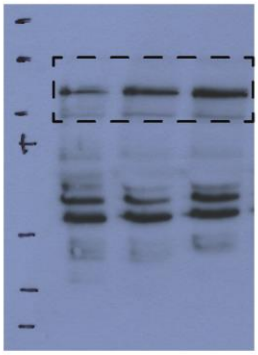

S18B
WB: TUBA

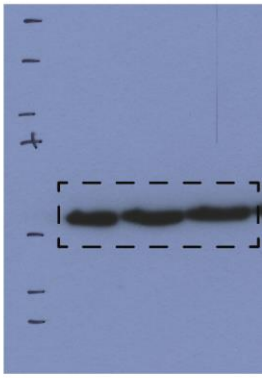

S18C
WB: p-MLC

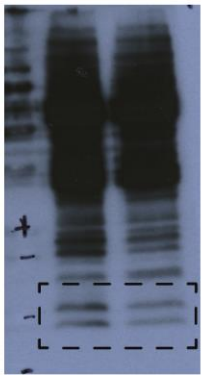

S18C
WB: MLC